Bioresource Technology Reports 34 (2026) 102658

Contents lists available at ScienceDirect

Bioresource Technology Reports

journal homepage: www.sciencedirect.com/journal/bioresource-technology-reports

Thermal valorisation of sewage sludge into artificial aggregates: A critical review of processes, environmental performance, and circular bioeconomy implications

Kannan Thushanthan [a,*], Muhammad Abdul Mannan [b], Muhammad Ekhlasur Rahman [a], Keerthan Poologanathan [a], Mujib Rahman [c]

[a] School of Engineering, Physics & Mathematics, Faculty of Engineering & Environment, Northumbria University, Newcastle-upon-Tyne, NE1 8ST, United Kingdom
[b] School of Civil Engineering, Faculty of Engineering, PNG University of Technology, LAE, 411, Morobe Province, Papua New Guinea
[c] Department of Civil Engineering, Aston University, B4 7ET, UK

ARTICLE INFO

Keywords:
Sewage sludge valorisation
Artificial lightweight aggregates
Circular bioeconomy
Resource recovery
Sintering
Heavy metals and PFAS immobilisation

ABSTRACT

The continuous generation of Sewage Sludge (SS) from wastewater treatment plants poses major environmental and management challenges while offering significant opportunities for bioresource valorisation. This review critically analyses the transformation of SS into Artificial Aggregates (AAs) through thermal processes such as sintering, highlighting its potential as a sustainable route for resource recovery and circular bioeconomy integration. The unique physicochemical composition of SS rich in SiO_2, Al_2O_3, CaO, Fe_2O_3, and organic matter enables granulation, bloating, and vitrification during sintering, producing lightweight aggregates with densities below 1200 kg m^{-3} and compressive strengths above 6 MPa. Incorporating supplementary binders such as fly ash, rice husk ash, and Na_2SiO_3 optimises sintering behaviour, enhances densification, and reduces water absorption. High-temperature sintering (>1050 °C) effectively immobilises toxic metals including Cd, Cr, and Pb, ensuring leachate concentrations remain within European Waste Acceptance Criteria limits. Beyond technical performance, SS-derived AAs contribute to climate change mitigation by offsetting the extraction of natural aggregates, lowering carbon emissions, and enabling waste to resource pathways consistent with Sustainable Development Goals (SDGs 6, 12, and 13). This review consolidates more than 180 studies, providing a state-of-the-art synthesis of process optimisation, binder synergy, environmental safety, and techno-economic perspectives. Key research gaps related to energy efficiency, scalability, and long-term durability are identified to guide future innovations in integrating SS derived aggregates into sustainable water resource recovery and bioengineering systems.

1. Introduction

In recent years, ecological disruption, global climate change, depletion of natural resources, and energy shortages have become pressing concerns for humanity challenges expected to intensify in the coming decades. To mitigate these issues, the adoption of circular economic practices, the development of greener materials, the preservation of existing resources, the extension of material lifespans, and the promotion of carbon-conscious lifestyles represent viable strategies for sustainable development (Justin et al., 2025; Poblete et al., 2025; Tian et al., 2023; Wang et al., 2025; Xiao, 2018; Xiao et al., 2025). It is projected that by 2050, rapid industrialisation and population growth will generate approximately 27,000 million tonnes of waste annually (Taki et al., 2020). Among these, sewage sludge (SS) a byproduct of wastewater treatment constitutes a substantial portion. Consequently, increasing attention has been directed toward its utilisation within the framework of a circular economy (Chen et al., 2024; Georgi et al., 2022; Kominko et al., 2024; Ragi et al., 2022; Silva et al., 2020; Wang et al., 2022).

SS is produced as a secondary by-product during the mechanical and biological treatment of wastewater. It contains nutrient rich compounds such as potassium (K), phosphorus (P), and nitrogen (N), along with

* Corresponding author.
E-mail addresses: kannan.thushanthan@northumbria.ac.uk (K. Thushanthan), mohammad.mannan@pnguot.ac.pg (M.A. Mannan), muhammad2.rahman@northumbria.ac.uk (M.E. Rahman), keerthan.pologanathan@northumbria.ac.uk (K. Pologanathan), m.rahman19@aston.ac.uk (M. Rahman).

https://doi.org/10.1016/j.biteb.2026.102658
Received 1 November 2025; Received in revised form 9 February 2026; Accepted 21 February 2026
Available online 26 February 2026

decomposable organic matter including fibres (Kumar et al., 2025; Rajput et al., 2024; Sánchez and Martins, 2021; Seleiman et al., 2020). However, it may also contain pollutants and pathogens, such as microplastics, parasite eggs, microorganisms, and toxic organic or inorganic substances (Okeke et al., 2022; Sidhu et al., 2024; Yang et al., 2021b; Zhang et al., 2022). If inadequately treated or disposed of, SS can emit offensive odours and deplete dissolved oxygen (DO) levels in water bodies, thereby threatening aquatic life and disturbing ecosystems(Goto et al., 2025; Mateo-Sagasta et al., 2015; Sidhu et al., 2024). The handling and disposal of SS have thus become a critical environmental and public health issue due to increasing production volumes and associated hazards. Globally, SS production has shown a consistent upward trend. Within the European Union, urban wastewater sludge generation continues to rise (Mininni et al., 2015). Similar patterns are observed in Asia: Japan recorded a 170% increase in SS generation between 1990 and 2014 (Hong et al., 2009), while in China, production doubled between 2010 and 2017 exceeding 36 million tonnes per annum with a 6% annual growth rate (Yang et al., 2021b; Yu et al., 2023). These data indicate a rise in SS production, a trend that is expected to continue as living standards and population growth increase (Fytili and Zabaniotou, 2008). In the United Kingdom, SS production rose by 43% between 2012 and 2023, with around 12 million tonnes of wastewater processed daily (European Union, 2024; Water UK, 2025). Implementation of stricter wastewater treatment regulations in the EU between 1992 and 2005 further contributed to a 50% rise in sludge production, which increased by an additional 20% by 2010/2011 to reach 10.4 million tonnes of Dry Matter (DM) (Bagheri et al., 2023; Garrido-Baserba et al., 2015). Certain Central and Eastern European countries, such as Lithuania, Poland, and Hungary, experienced up to a 100% increase, reaching 2.5 million tonnes of DM due to differential compliance with wastewater directives

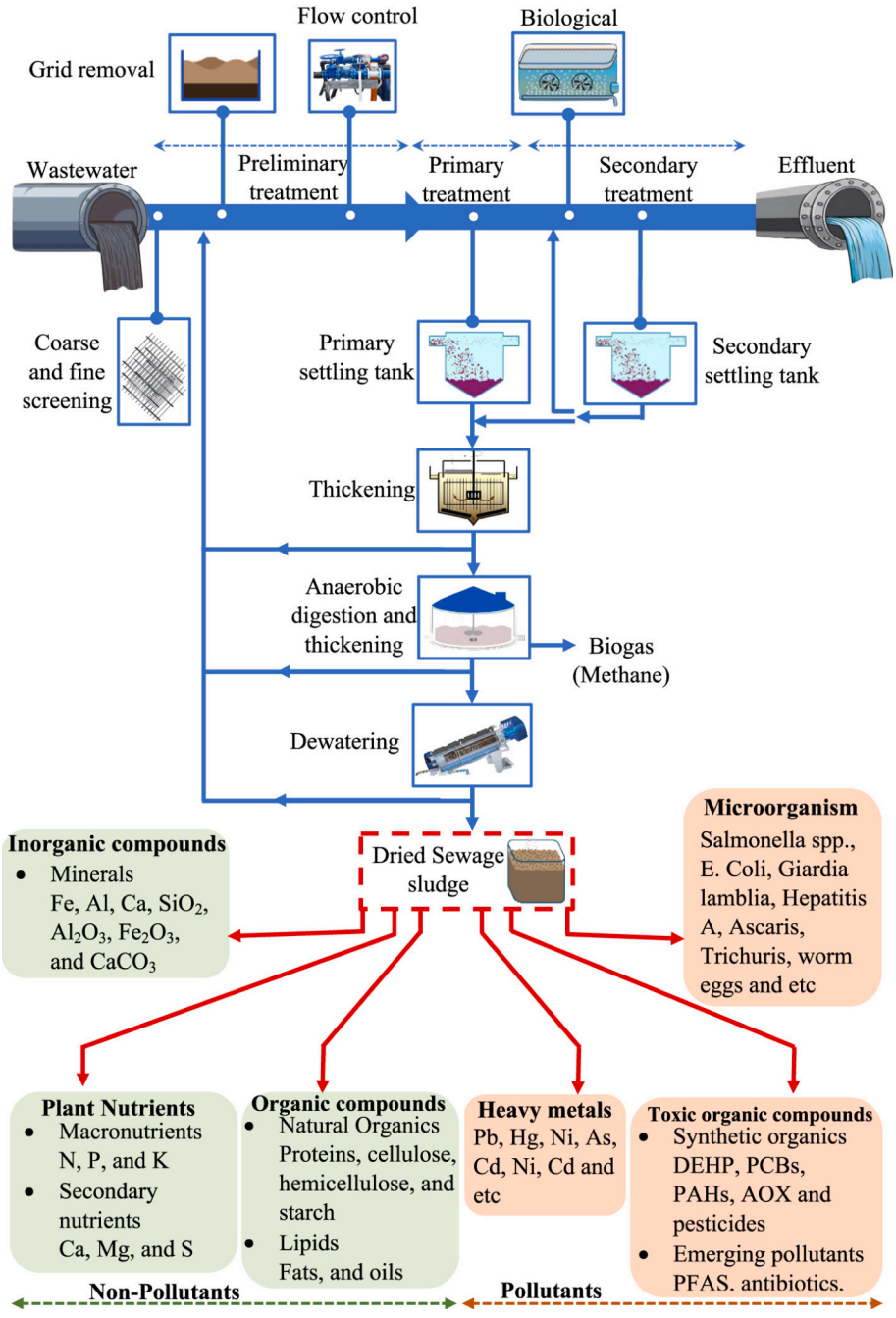

Fig. 1. Wastewater treatment process and components in dried sewage sludge.

(Bianchini et al., 2016; Collivignarelli et al., 2017; Grobelak et al., 2016; Świerczek et al., 2018). By 2020, Europe's total SS production was estimated at approximately 13 million tonnes, equivalent to 45–56 g of dry sludge per person per day (Mininni et al., 2015).

SS, produced as a byproduct of wastewater treatment, as seen in Fig. 1, chemically it comprises a complex mixture of organic matter and essential macronutrients (N, P, K), alongside micronutrients such as iron (Fe), zinc (Zn), and copper (Cu). These attributes make SS potentially valuable for agricultural applications, particularly in organic farming (Collivignarelli et al., 2019; Gao et al., 2020; Ye et al., 2022). However, its composition varies considerably depending on treatment processes and wastewater characteristics, complicating its direct use as fertiliser. Contamination by heavy metals, pathogens, and persistent organic pollutants remains a key concern. Studies report that 50–80% of the heavy metals in wastewater persist within the sludge matrix (Li and Zhang, 2021; Yang et al., 2020). Posing risks of bioaccumulation and entry into the food chain when applied to land (Chagas et al., 2021). Although some heavy metals may be present in very low concentrations, prolonged consumption of products grown on these farmlands can result in serious health issues, particularly kidney and bone diseases. Furthermore, certain heavy metals, such as arsenic (As), mercury (Hg), and lead (Pb), can be toxic even at minor concentrations. The toxicity of these metals can adversely affect neurological and cardiovascular functions (Kanwar et al., 2023; Li and Zhang, 2021).

To mitigate such risks, the safe use of SS for land application is governed by regulatory frameworks such as EU Directive 86/278/EEC (Bagheri et al., 2023; Council of the European Communities, 1986). which specifies permissible heavy metal concentrations (mg/kg DM): Zn 2500–4000, Cu 1000–1750, Pb 750–1200, Ni 300–400, Hg 16–25, and Cd 20–40. Some countries have adopted even stricter standards, resulting in declining heavy metal levels over time (Sidhu et al., 2024). Industrial wastewater and road surface runoff are major contributors to SS contamination, whereas sludge from smaller, domestically fed treatment plants typically exhibits lower pollutant levels (Duan et al., 2017; Praspaliauskas and Pedišius, 2017). When major directives such as 40 CFR Part 503(A, 1994) and Directive 86/278/EEC (Council of the European Communities, 1986) were established, contaminants of emerging concern (CECs) such as per and polyfluoroalkyl substances (PFAS), micro and nano plastics (MNPs), and pharmaceutical residues were largely unrecognised. However, modern studies have revealed their prevalence and potential ecological hazards (Xue et al., 2025). A recent U.S. EPA survey detected more than 700 chemical compounds in biosolids, including pharmaceuticals, personal care products, and industrial chemicals (Richman et al., 2022). Among these, PFAS comprising over 15,000 synthetic organo-fluorine compounds or their degradation products. These chemicals are amphiphobic and highly resistant to chemical and thermal breakdown, earning them the label "forever chemicals." Due to these unique properties, PFAS are widely used in household products such as detergents, non-stick cookware, and carpets, as well as in industrial applications. Long-chain legacy PFAS, in particular, are known to be harmful to human health, wildlife, and aquatic ecosystems. Given these risks, there is growing momentum toward introducing stricter regulations and environmental policies, signalling a shift in future biosolid management practices (Xue et al., 2025).

Given its complex and potentially hazardous composition, SS management represents a major sustainability challenge. Existing management strategies can be broadly classified into four categories: (i) disposal, (ii) land application, (iii) energy recovery, and (iv) sludge-based product development (Bagheri et al., 2023). Fig. 2. Presents a detailed summary of the SS management methods comparing the risk challenges and recent trends in each method. Historically, disposal methods such as landfilling and ocean dumping were commonly utilised for the management of SS (Aubain et al., 2002; Heap et al., 1991). However, growing environmental and regulatory pressures including concerns over heavy metal leaching, greenhouse gas emissions, and pathogen transmission have led to their gradual decline (International Maritime Organisation(IMO), 2022; Liu et al., 2022; National Oceanic

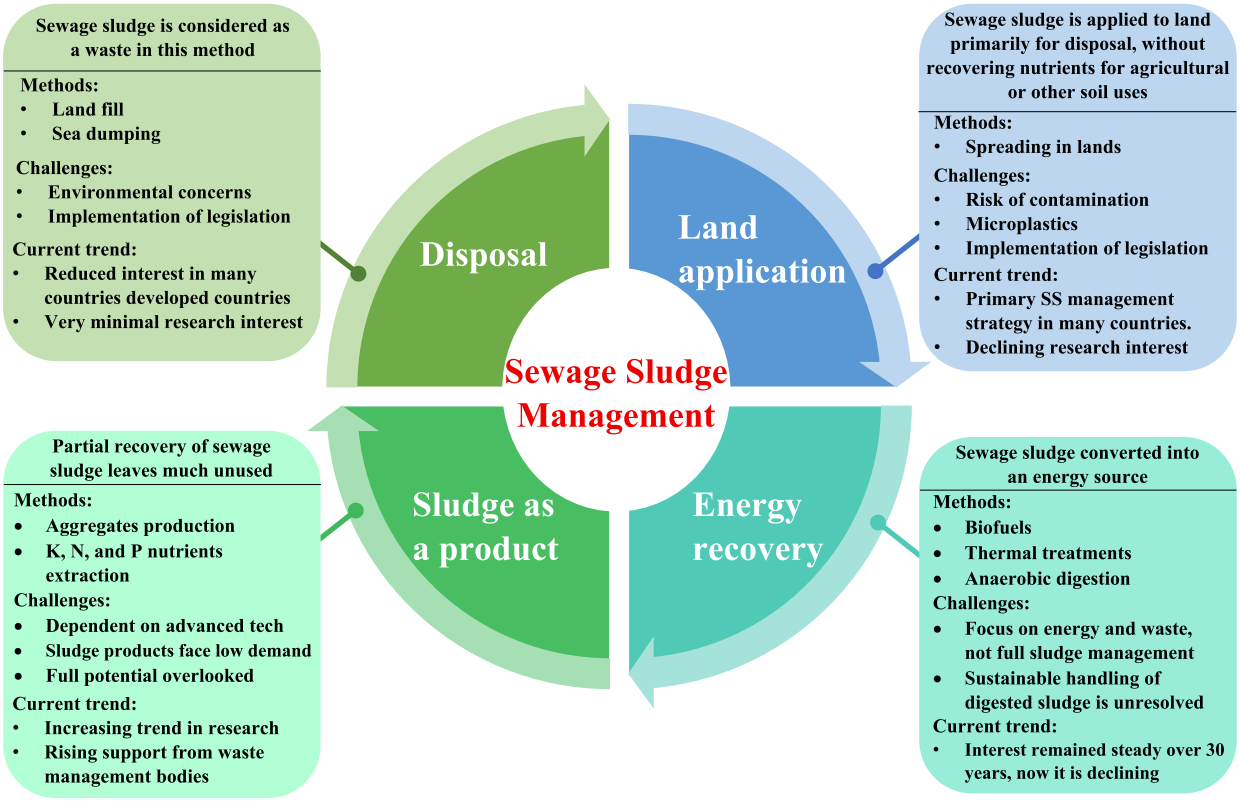

Fig. 2. Sewage sludge management strategies, methods, challenges and current trends.

and Atmospheric Administration(NOAA), 2001). Despite this, approximately 10% of SS in the European Union is still landfilled (Buta et al., 2021; European Environment Agency, 2024). Alternative approaches, such as energy recovery and agricultural reuse, have gained traction. Energy recovery processes aim to reduce sludge volume while generating energy through incineration, pyrolysis, or gasification (Bagheri et al., 2023; Capodaglio and Callegari, 2023; Meena et al., 2019; Sidhu et al., 2024). In land application, SS is treated as a resource and utilised in agriculture for crop production and farm activities(Buta et al., 2021; Fytili and Zabaniotou, 2008; Kominko et al., 2024). Compared to landfilling, this approach treats SS as a value-added product. However, concerns remain regarding the presence of heavy metals, organic pollutants, pathogens, and microplastics, making its suitability a key topic in ongoing research (Poinen and Bokhoree, 2022; Sakali et al., 2021). More recently, the sludge-based product method focuses on extracting specific compounds from SS for the production of useful materials has emerged as a promising strategy. Focusing on extracting valuable compounds or repurposing SS into secondary materials such as fertilisers, catalysts, artificial aggregates (AAs), and construction products including bricks and pavers this approach has gained popularity as it offers a sustainable alternative to depleting natural resources (Fytili and Zabaniotou, 2008; Goto et al., 2025; Ji et al., 2023; Lau et al., 2017; Massa et al., 2025; Świerczek et al., 2018). These advancements underscore the potential of SS as a valuable resource, reinforcing the need for innovative and environmentally friendly management solutions. Utilising SS for the formulation of AA provides sustainable solution for the increasing SS generation and associated management concerns, and the depletion of natural aggregate due to the rapid growing construction sector.

The construction industry remains a major environmental contributor, responsible for high energy consumption, resource depletion, and approximately one tonne of CO_2 emissions per tonne of Portland cement produced (Hasheminezhad et al., 2024). Rapid urbanisation and population growth continue to increase the demand for concrete and aggregates. For example, China's cement consumption, a proxy for aggregate demand has surged by 438% in the past two decades, compared with a global average increase of 60% (Peduzzi and Peduzzi, 2014). Current global aggregate consumption is estimated between 32 and 50 billion tonnes per year (UNEP et al., 2016). This rising demand underscores the urgent need to identify sustainable aggregate alternatives.

The simultaneous challenges of aggregate scarcity and sludge overproduction present a unique opportunity to integrate SS into construction materials, particularly as AAs. Such valorisation strategies align with the United Nations Sustainable Development Goals (SDGs) notably SDG 12 (Responsible Consumption and Production) and SDG 13 (Climate Action) by promoting resource efficiency, waste reduction, and reduced greenhouse gas emissions.

Accordingly, the primary objective of this review is to comprehensively evaluate the potential of SS for AA production and to consolidate emerging insights into process optimisation for sustainable and economically viable manufacturing. While several previous reviews have explored the use of waste derived materials as aggregate substitutes, these studies have largely focused on material characterisation or individual processing techniques, with limited attention to energy demand, environmental performance, and comparative evaluation of alternative production routes. In particular, the specific potential of SS based aggregates, when assessed within an integrated framework encompassing processing mechanisms, performance behaviour, and techno economic considerations, remains underexplored. This review addresses these gaps by systematically examining the morphological, physical, and chemical characteristics of SS that govern aggregate performance, alongside a critical assessment of mechanical, durability, energy, and environmental outcomes. Emphasis is placed on process optimisation strategies including sintering conditions, material blending, and granulation parameters as well as on comparative analysis with low temperature aggregate production routes. By integrating these aspects, this review provides a holistic and critical assessment of SS valorisation for aggregate production, thereby offering clear guidance for future research and supporting sustainable waste management and resource recovery within a circular economy framework.

2. Review methodology

This review adopts a structured and systematic approach to ensure a comprehensive and unbiased synthesis of global research on the utilisation of SS for AA production. The methodology comprised several key stages, including the definition of research scope, database selection, screening of relevant literature, critical evaluation, and thematic synthesis. The literature search was conducted across major scientific databases, namely Scopus, Web of Science, Google Scholar, ASCE Library, Taylor & Francis Online, Wiley Online Library, and ScienceDirect, encompassing studies published between 2000 and 2025 within the fields of engineering, materials science, and environmental science.

To capture the most relevant literature, a combination of keywords and Boolean operators was employed, including “sewage sludge”, “artificial aggregate”, “lightweight aggregate”, “sintered aggregate”, “cold-bonded aggregate”, “waste valorisation”, and “circular economy”. Irrelevant search terms such as “recycled aggregate”, “asphalt”, and “artificial intelligence” were excluded to refine the dataset. The initial search retrieved approximately 9000 peer reviewed publications from over sixty journals, of which duplicates, and non-relevant records were removed. Titles, abstracts, and conclusions were then screened to identify studies that directly addressed the processing, performance, or environmental implications of SS based aggregates. This process yielded 430 potentially relevant studies, which were subsequently subjected to full text evaluation. After detailed assessment, 180 papers meeting the inclusion criteria were retained for in-depth analysis.

Each selected paper was examined to extract data concerning the physicochemical composition of SS, sintering and cold-bonding parameters, mechanical and environmental performance, and sustainability indicators. Bibliometric and co-occurrence analyses were performed using VOSviewer software to identify research trends, frequently co cited authors, and emerging themes. The final body of literature was organised into four primary thematic areas: (1) material characteristics of SS, (2) processing and sintering mechanisms, (3) mechanical, physical, and environmental performance, and (4) socio economic and circular economy perspectives. This structured methodology ensures transparency, reproducibility, and scientific rigour in synthesising the state of knowledge surrounding SS based artificial aggregates.

3. Suitability of sewage sludge for artificial aggregate production

The utilisation of SS as a secondary product has gained increasing attention over the past two decades and continues to expand globally. Among its diverse valorisation pathways, aggregate production from SS presents considerable economic and environmental advantages, attracting substantial research interest (Khanbilvardi and Afshari, 1995; Korol et al., 2020; Lau et al., 2018; Laursen et al., 2006; Mun, 2007). The inherently high organic content of SS generates significant volumes of gas during thermal processing (sintering), which not only promotes pore formation and reduces bulk density but also lowers the energy demand during production (Chiou et al., 2006a; Forth et al., 2015). This phenomenon facilitates the creation of lightweight artificial aggregates (LWA) from SS, offering a sustainable alternative to natural aggregates while mitigating environmental concerns associated with resource depletion and ecological disturbance.

The suitability of SS for AA production depends on its performance across the two principal stages of AA manufacturing: granulation and hardening (Ren et al., 2021).

3.1. Granulation process

The granulation process involves the preparation of green granules from fine raw materials prior to hardening. Two main techniques are employed: agitation granulation and compaction granulation. Among these, agitation granulation is the most commonly adopted due to its simplicity and energy efficiency (Chiou et al., 2006a; Huang and Wang, 2013; Ren et al., 2021; Shi et al., 2019). In agitation granulation, raw materials are tumbled in a rotary drum or disc pelletiser without the application of external compaction forces. The moisture content within the raw materials promotes adhesion through capillary pressure, surface tension, and viscous forces, allowing the particles to coalesce into spherical green pellets (Suresh et al., 2016a). At this stage, the pellets have limited mechanical strength and must be handled carefully during drying, storage, and transport. Their initial strength derives primarily from particle interlocking and cohesive forces induced by surface tension, which together form a dense outer layer stabilising the pellets (Arslan and Baykal, 2006). The characteristics of green pellets are influenced by two key groups of factors:

1. **Raw material properties**, including particle fineness, moisture content, and the presence of binders (Arslan and Baykal, 2006; Geetha and Ramamurthy, 2010a; Lau et al., 2017; Manikandan and Ramamurthy, 2007)
2. **Mechanical process parameters**, such as granulation time, rotation speed, and inclination angle of the pelletiser (Shi et al., 2019; Tajra et al., 2018)

Material fineness plays a critical role in granulation efficiency. Manikandan and Ramamurthy (2007) reported that increasing the specific surface area of fly ash from 257 m^2/kg to 414 m^2/kg enhanced the conversion rate of raw materials into aggregates from 12% to 100%. Similarly, adequate moisture retention is essential to develop cohesive forces within the mix. Harikrishnan and Ramamurthy (2006) observed that maintaining a moisture content between 15% and 35% yields uniform aggregates with consistent size distribution. In contrast, compaction granulation involves the application of mechanical pressure to compact the raw materials into dense granules, which are subsequently rolled into spherical pellets (Ren et al., 2021). This technique is suitable for producing aggregates with more uniform dimensions, typically between 8 and 10 mm. The primary parameters affecting the mechanical properties of compaction-based granules include the moisture content of the feedstock and the applied compaction stress (González-Corrochano et al., 2009a; Liao and Huang, 2011; Tsai and Li, 2012).

3.2. Hardening process

The hardening process transforms the freshly prepared green pellets into mechanically stable aggregates. Among the various hardening methods, sintering remains the most widely used in commercial aggregate production and was first developed in the United Kingdom during the mid twentieth century (Ren et al., 2021) However, alternative techniques such as cold bonding and alkaline activation have recently emerged as sustainable and energy efficient options (Rashad, 2018). Sintering involves heating the green pellets to temperatures typically above 1000 °C, promoting particle fusion at points of contact and producing dense, hardened aggregates with enhanced strength and durability (Ramamurthy and Harikrishnan, 2006).Two key phenomena govern the sintering of sludge-based aggregates: expansion and vitrification. Expansion results from the release of gases generated at elevated temperatures a process commonly referred to as bloating which creates internal pores and reduces density. Vitrification, in contrast, forms a dense, glassy, and crystalline matrix by melting the material's surface and sealing internal voids (Lau et al., 2017; Liu et al., 2018a). Together, these processes determine the final microstructure and performance of the aggregate. Sintering is a complex process influenced by both material composition and processing parameters such as temperature, heating rate, and dwell time (Ren et al., 2021). According to González-Corrochano et al. (2009a) the feedstock must contain sufficient organic matter to generate gas during sintering, a property reflected in its loss on ignition (LOI) value. Moreover, materials should exhibit pyroplasticity the ability to soften and deform under their own weight at high temperatures coinciding with gas generation. The synchronisation of pyroplasticity and gas evolution ensures that the expanding gases remain trapped within a vitrified surface layer, producing aggregates with optimal porosity and mechanical strength.

3.3. Surface morphology of sewage sludge

The surface morphology of SS plays a crucial role in determining its suitability for AA production. Scanning Electron Microscope (SEM) images of SS particles reported in the literature as shown in Fig. 3(a). reveal irregular and highly porous surfaces, with particles agglomerated and adhered to fibrous structures. Such irregular morphologies promote mechanical interlocking between particles an essential mechanism contributing to the initial strength of green pellets during handling and storage, as illustrated in Fig. 3(a)-v. Similar observations have been reported by several studies, which identify fibrous biomass structures as the principal binding mechanism in densified products (Molenda et al., 2021). Lau et al. (2017) reported that SS particles typically exhibit mean diameters ranging from 20.83 μm to 48.75 μm, accompanied by a specific surface area of approximately 2675 m^2/kg. This high fineness enhances the reactivity and cohesion of SS when used as a raw material for AA production. Moreover, the elevated organic and fibrous content of SS confers substantial moisture retention capacity, a property that supports the development of cohesive forces during pelletisation and aggregate formation. This moisture behaviour is attributed to the flocculent molecular structure of organic matter, particularly its prevalence in the ionic form of fulvic acid, which readily adheres to particle surfaces to form an adsorption film. These films enhance the capacity for water absorption and retention, thereby improving particle cohesion and plasticity during pellet formation (Fig. 3(b)) (Ruimin et al., 2021). Consequently, the organic matter in SS facilitates the formation of spherical green pellets with adequate integrity prior to hardening.

However, these same characteristics can also hinder granulation efficiency. The adsorption of fine particles onto organic films may obstruct infiltration channels, reducing permeability, while the extensive specific surface area of organic matter promotes the formation of bound water films that impede drainage and consolidation (Fig. 3(b)). As a result, excessive organic content can increase material compressibility, reducing the overall stability of green pellets and complicating the formation of uniformly granulated aggregates (Tuncel and Pekmezci, 2018).

In summary, the surface morphology of SS characterised by its irregular, fibrous, and porous nature offers both advantages and challenges for AA production. While these features enhance interparticle bonding and moisture retention during granulation, they can simultaneously compromise pellet strength and structural uniformity if the organic content is excessive. Optimising the organic-to-inorganic ratio in SS, therefore, remains essential to balance cohesion and drainage, ensuring the formation of structurally stable aggregates suitable for sintering.

3.4. Physical properties of sewage sludge

The physical properties of SS are key determinants of its performance and suitability in AA production. Chiou et al. (2006b) reported that SS exhibits a LOI compared with other commonly utilised raw materials such as fly ash and pulverised fuel ash. A high LOI indicates a greater proportion of volatile organic matter, which generates gas during thermal processing (sintering). This gas formation promotes pore development, resulting in porous, lightweight aggregates with reduced density

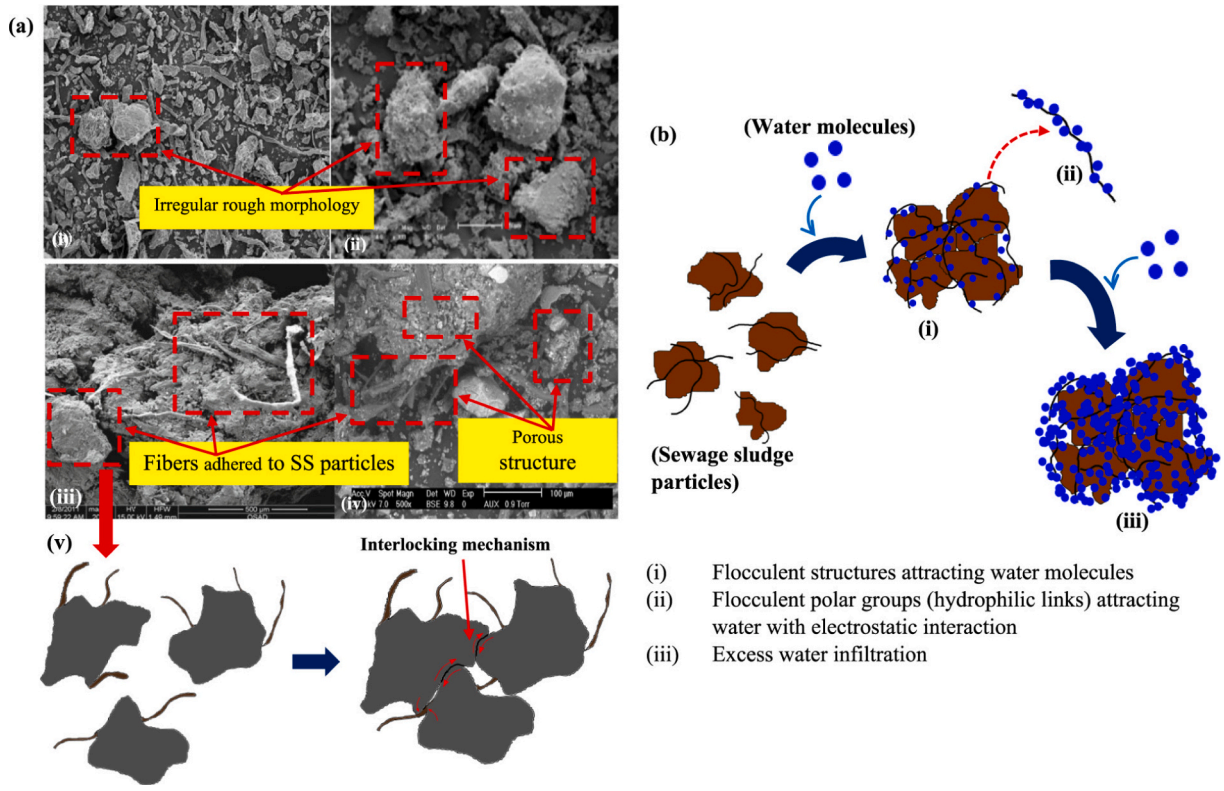

Fig. 3. Microstructure and water retention mechanisms of sewage sludge: (a) (i, ii, iii, iv) SEM images of SS particles (Ábrego et al., 2009; Lima et al., 2015; Ramamurthy and Harikrishnan, 2006; Torri et al., 2014) (v) Schematic diagram of particle interlocking mechanism in SS (b) schematic illustration of water attachment due to flocculent structure.

an essential characteristic of LWA. Consequently, the thermal decomposition behaviour of SS significantly influences both the efficiency and quality of AA production. Several studies have employed thermogravimetric analysis (TGA) and differential thermal analysis (DTA) to examine the decomposition characteristics and LOI behaviour of SS (Franus et al., 2016; Lau et al., 2017; Magdziarz et al., 2011). The TG-DTA curve provides insights into the thermal stability, decomposition kinetics, and phase transitions of materials during heating, by monitoring mass changes and associated thermal effects. Distinct peaks on the curve correspond to decomposition reactions, gas evolution, and glass-phase formation critical phenomena that define the gas-forming behaviour of SS during sintering. A representative TG-DTA curve for SS provided in the supplementary materials (Fig. S1(a)).

The TG-DTA profile typically displays multiple decomposition peaks, each corresponding to specific physical or chemical transformations. The initial peaks (P1 and P2) reflect moisture evaporation, attributed to the high inherent water content of SS (Zheng and Koziński, 2000). The exothermic peak P3 corresponds to the combustion of organic compounds, generating CO_2 and leading to noticeable mass loss. The subsequent P4 peak represents the combustion of weddellite ($CaC_2O_4{\cdot}2H_2O$) and further mass reduction due to CO release. An endothermic reaction at P6 marks the decomposition of calcium carbonate ($CaCO_3$), accompanied by rapid mass loss as CO_2 gas is released (Othuman and Wang, 2011). The final P7 peak is linked to the breakdown of alkali metal sulphates, signifying the completion of major thermal decomposition events (Lau et al., 2017). A schematic representation of the combustion and decomposition stages of SS during sintering is shown in supplementary materials (Fig. S1 (b)).

Based on TG-DTA analysis, the principal gas forming reactions during the thermal treatment of SS include:

1) Loss of free and bound water
2) Combustion of organic matter
3) Decomposition of calcium carbonate and calcium oxalate hydrates
4) Chemical reactions leading to particle melting and fusion
5) Decomposition of alkali metal sulphates

The cumulative effect of these reactions facilitates gas evolution, a crucial phenomenon for the formation of expanded, low-density AAs.

Furthermore, X-ray diffraction (XRD) analyses have identified mineral phases such as quartz, portlandite, calcite, and weddellite as predominant in SS (El-Deen and Zhang, 2012; Torri and Lavado, 2008). At elevated temperatures, quartz transitions into a viscous glassy phase, while CaO generated from calcite decomposition releases CO_2 gas, contributing to the formation of a lightweight, porous structure. This combined effect enhances the specific strength and structural integrity of the resulting aggregates (Chen et al., 2010). LWA are generally defined as granular materials with a loose bulk density below 1200 kg/m^3 and oven-dry particle density below 2000 kg/m^3 (Lau et al., 2017). These materials offer significant advantages over conventional aggregates, including reduced dead load on structures, lower foundation and reinforcement requirements, and decreased transportation costs. Cheeseman and Virdi (2005) outlined the desirable characteristics of high quality LWA as follows:

1. A strong, sintered ceramic core with low density and internal porosity
2. A dense outer shell exhibiting minimal water absorption
3. A nearly spherical geometry that enhances workability and reduces edge effects in fresh concrete.

Chiou et al. (2006) further noted that SS-derived aggregates possess lower bulk density and, due to their high organic content, can achieve energy efficient sintering at reduced temperatures. This thermal efficiency arises from the exothermic combustion of organics within the sludge matrix, which partially offsets the external energy input required for sintering.

In summary, the physical and thermal characteristics of SS specifically its high LOI, favourable gas-forming behaviour, and mineralogical composition demonstrate strong potential for producing lightweight, porous aggregates under controlled sintering conditions. These properties not only facilitate the production of sustainable AAs but also contribute to energy conservation and material circularity in the construction sector.

3.5. Chemical properties of sewage sludge

The chemical composition of raw materials fundamentally governs the viscosity, melting behaviour, and sintering characteristics of AAs. The major oxides present silicon dioxide (SiO_2), aluminium oxide (Al_2O_3), and calcium oxide (CaO) play distinct roles in determining these properties. SiO_2 and Al_2O_3 form a polymeric silicate-aluminate network that increases viscosity and stabilises the molten phase, while fluxing oxides such as CaO, Fe_2O_3, Na_2O, and K_2O act as network modifiers, lowering viscosity and softening temperatures(Lau et al., 2017). During sintering, materials with high SiO_2 and Al_2O_3 contents tend to form a highly viscous, adhesive glassy phase capable of trapping gases released from organic decomposition (bloating). This promotes the formation of a dense vitrified outer shell enclosing a lightweight porous core, thereby enhancing aggregate strength and reducing water absorption (Adell et al., 2007; Yue et al., 2011b). Conversely, excessive CaO combined with insufficient SiO_2 can hinder vitrification, leading to weak shell formation, excessive porosity, and reduced mechanical performance (Lau et al., 2017). The expansion and vitrification mechanisms occurring during SS-based AA sintering, and the resulting internal microstructure, are illustrated in Fig. 4. The suitability of SS as a precursor material is often evaluated using oxide mass ratios, particularly SiO_2/Σ(Flux elements) and $\Sigma(SiO_2 + Al_2O_3)/\Sigma$(Flux elements), where flux elements comprise CaO, Fe_2O_3, Na_2O, K_2O, and MgO. A higher SiO_2/Σ(Flux elements) ratio (>2) promotes stability and reduces excessive melting, while maintaining $\Sigma(SiO_2 + Al_2O_3)/\Sigma$(Flux elements) between 3.5 and 10 ensures sufficient gas entrapment and optimal sintering behaviour (Chen et al., 2010; de' Gennaro et al., 2004; González-Corrochano et al., 2009a). Elevated flux contents lower the softening temperature, but excessive amounts may lead to uncontrolled expansion and poor aggregate integrity.

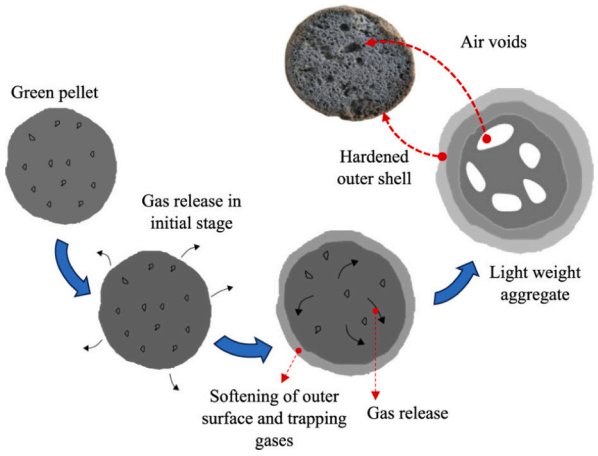

Fig. 4. SS aggregate internal structure change during sintering process and comparison with published research study (Huang and Wang, 2013).

The Riley (1951) is frequently used to predict the bloating potential of raw materials based on their oxide composition. This ternary diagram defines a "bloating region", representing the optimal compositional range for materials capable of stable expansion during sintering. Materials falling within this region typically exhibit SiO_2 contents of approximately 48–70 wt%, Al_2O_3 contents of 8–25 wt%, and Fe_2O_3 contents of 3–12 wt%, ensuring adequate glass-phase formation and melt viscosity control. In addition, the presence of alkaline and alkaline-earth fluxes, commonly expressed as CaO + MgO in the range of 1–12 wt % and $Na_2O + K_2O$ in the range of 0.5–7 wt%, is critical for reducing softening temperatures and facilitating gas entrapment within the viscous melt. Raw materials whose overall oxide compositions fall within these compositional windows are therefore considered well suited for producing bloated, LWA with stable pore structures during high-temperature sintering.

The chemical compositions of SS reported in various studies on AA production are summarised in Table 1, along with mean values and standard deviations. The primary constituents SiO_2, Al_2O_3, Fe_2O_3, and CaO collectively account for approximately 66% of the total dry mass of SS. However, their relative proportions vary considerably depending on

Table 1
Reported chemical compositions of sewage sludge used in artificial aggregate studies (Andrzejuk et al., 2024; Dang et al., 2023; Lau et al., 2017; Li et al., 2016; Li et al., 2020a; Min Wie et al., 2023; Mun, 2007; Ramadan et al., 2008; Souza et al., 2020; Thukkaram and Arun Kumar, 2024; Tuan et al., 2013; Wang et al., 2009b).

Oxide Component	Reported Range (wt%)	Mean (wt%)	Standard Deviation (±)	Relevance to Aggregate Formation
SiO_2	6.08–52.00	27.36	15.39	Primary glass former that promotes vitrification and the formation of a dense outer shell during sintering
Al_2O_3	2.40–20.94	11.17	6.35	Enhances melt viscosity and structural stability
Fe_2O_3	1.27–48.51	11.92	12.35	Acts as a fluxing agent, promoting bloating behaviour and contributing to colour development during sintering
CaO	2.63–41.53	11.22	10.92	Acts as a flux, lowering the softening temperature and influencing strength development and pore structure during sintering
MgO	0.63–10.68	3.13	3.23	Acts as a secondary flux, influencing melt behaviour
Na_2O	0.00–2.30	0.55	0.72	Acts as an alkali flux, reducing the melting temperature
K_2O	0.11–7.82	2.31	2.28	Acts as an alkali flux, promoting vitrification
SO_3	0.22–11.00	4.27	4.08	Acts as a gas forming component, contributing to bloating through gas release during sintering
P_2O_5	5.31–32.98	14.84	9.49	Influences glass network and melt chemistry
TiO_2	0.41–1.40	0.88	0.38	A minor oxide, contributing to crystallisation
MnO	0.11–0.12	0.12	0.01	A trace flux oxide with a minor influence on melt behaviour during sintering

factors such as wastewater source, treatment process, and sludge type (Sidhu et al., 2024). When compared with the optimal compositional ranges for bloating materials, most SS samples exhibit suitable levels of Fe_2O_3, CaO + MgO, and K_2O + Na_2O, whereas SiO_2 and Al_2O_3 are often lower than ideal. To address these deficiencies, researchers have explored the addition of silica and alumina rich supplementary materials including Palm Oil Fuel Ash (POFA) (Lau et al., 2017), fly ash (Liu et al., 2012), rice husk ash (Souza et al., 2020), clay (Xu et al., 2006), and binders (Lau et al., 2017; Manikandan and Ramamurthy, 2007) to optimise SS feedstock composition. Among chemical additives, sodium silicate (Na_2SiO_3) is particularly effective, as it enhances the formation of glassy phases and improves aggregate strength through its high SiO_2 contribution (Jo et al., 2007; Xu et al., 2008, 2006). Similarly, coal ash is frequently incorporated to increase the SiO_2 and Al_2O_3 content, thereby improving mechanical strength and sintering performance (Wang et al., 2009a). Other effective binders reported in the literature include bentonite (Manikandan and Ramamurthy, 2007), glass powders (Kockal and Ozturan, 2011), and lime (Ramamurthy and Harikrishnan, 2006) which modify surface chemistry and enhance cohesion during pelletisation.

Overall, the chemical composition of SS demonstrates promising potential for AA production, particularly when appropriately blended with corrective additives. The balance between silica, alumina, and flux oxides dictates the degree of expansion, vitrification, and structural stability, ultimately determining aggregate quality.

4. Sewage sludge based aggregate production

The production of sintered SS based aggregates involves homogeneous mixing of SS with supplementary materials to achieve the target chemical composition (Section 3.5), followed by agitation and sintering. As discussed in Section 3.2, agitation technique is widely adopted for pelletising SS based materials at both laboratory and industrial scales.

In this process, raw materials are fed into a rotary drum or disc pelletiser and subjected to continuous rotation, which promotes particle collision, adhesion, and subsequent granulation. Pelletisation generally occurs in two stages.

1. **Stage 1:** Dry mixing of raw materials for 2–3 min to ensure homogeneity.
2. **Stage 2**: Gradual addition of approximately 75% of the total water or liquid binder to initiate agglomeration, followed by spraying of the remaining moisture to act as a wetting agent, facilitating rolling and spherical pellet formation.

The efficiency of pelletisation and the size distribution of the resulting aggregates are primarily influenced by three operational parameters: the inclination angle (IA) of the disc, the rotational speed, and the duration of rotation (Bekkeri et al., 2023). Adjusting the IA and rotational speed directly affects capillary attraction between particles, thereby influencing pellet growth and uniformity. Reported studies indicate that IA values between 35° and 55° yield favourable results for AA production (Bekkeri et al., 2023; Harikrishnan and Ramamurthy, 2006; Risdanareni et al., 2020; Shivaprasad and Das, 2021). Exceeding 55° can cause aggregate collapse due to excessive gravitational forces, while angles below 35° typically result in small, weakly bound particles (2–4 mm) (Ren et al., 2021).

Similarly, rotational speed plays a decisive role in granulation behaviour. At lower speeds, gravitational forces dominate, resulting in sluggish movement and limited cohesion, whereas at higher speeds, centrifugal forces become excessive, leading to pellet disintegration (Bekkeri et al., 2023; Harikrishnan and Ramamurthy, 2006). Therefore, an optimal balance between these forces is required. Previous studies recommend rotational speeds between 30 and 60 rpm (Colangelo et al., 2015; Shivaprasad and Das, 2021; Vasugi and Ramamurthy, 2014). Tian et al. (2021) identified 40° IA and 55 rpm as optimal conditions, while Shi et al. (2019), proposed a range of 40°-45° IA for stable performance. For staged mixing, Tian et al. (2021) recommended initiating at 30 rpm and increasing to 55 rpm in Stage 2. Several other studies also reported that speeds between 35 and 55 rpm yield higher palletisation efficiency (Baykal and Döven, 2000; Ren et al., 2021; Shivaprasad and Das, 2021). Additionally, an IA of 42° combined with a rotational speed of 45 rpm has been shown to further enhance palletisation efficiency(Gesoğlu et al., 2012; Ren et al., 2021). Bekkeri et al. (2023) suggested maintaining total pelletisation duration within 20 min, with 10–15 min typically sufficient for uniform aggregate formation a finding corroborated by other studies (Kockal and Ozturan, 2011; Risdanareni et al., 2020; Vasugi and Ramamurthy, 2014).

Following pelletisation, green aggregates must be handled cautiously due to their limited mechanical integrity. Prior to sintering, they are typically air-dried under ambient conditions for approximately 24 h, followed by preheating to remove residual moisture and volatile compounds, thereby preventing flash heating and structural damage. Omitting this step can result in aggregate cracking or explosion (Lo et al., 2016; F. Yang et al., 2023). A preheating regime of 15–20 min at 300–400 °C is generally recommended, providing enhanced mechanical performance while maintaining energy efficiency (Yue et al., 2011a). However, it should be noted that reported preheating temperatures, dwell times, and subsequent sintering conditions vary considerably across studies. This variability reflects differences in SS composition, organic matter content, supplementary material chemistry, pellet size distribution, heating rate, and furnace configuration.

The sintering stage involves firing at temperatures typically exceeding 1000 °C to induce vitrification and expansion, producing hardened aggregates. Controlled slow cooling following sintering is essential to minimise thermal shock and microcrack formation. Zhang et al. (2015) reported that rapidly cooled aggregates exhibited compressive strength up to five times lower than those subjected to gradual cooling. A summary of experimental studies investigating SS-based AA production, covering raw materials, sintering conditions, and testing parameters, is presented in Table 2.

5. Properties of sintered sewage sludge based aggregates

The main mechanical and durability properties of sintered SS aggregates include:

1) Bulk and particle density
2) Water absorption
3) Shrinkage index
4) Crushing strength.

According to Lau et al. (2017), these properties are primarily governed by the proportions of raw materials, sintering temperature, and binder composition. The following subsections discuss how these factors influence the performance of AA.

5.1. Bulk density, and particle density and shrinkage

Bulk density and particle density are key parameters for classifying aggregates as LWA. According to EN 13055–1 (2002), aggregates with a bulk density below 1200 kg/m^3(1.2 g/cm^3) or a particle density below 2000 kg/m^3(2.0 g/cm^3) are classified as LWA (Souza et al., 2020). The density of an aggregate is primarily influenced by its bloating behaviour, which depends on the composition and proportion of flux elements in the raw mix. Clays and SS typically produce aggregates of lower density than fly ash, owing to their higher contents of iron oxides and carbon, which enhance bloating through gas generation during sintering. In contrast, fly ash contains fewer flux elements and greater proportions of high-melting-point oxides (SiO_2 and Al_2O_3), limiting its expansion potential Ren et al. (2021). Yue et al. (2011b) compared aggregates produced from fly ash clay mixtures with those containing clay and SS,

Table 2
Summary of representative experimental studies on SS based sintered AAs.

Raw materials used	Mixes / variations	Pre-sintering heating conditions	Sintering temperature (°C)	Sintering time (min)	Variables compared	Tests conducted	Reference
SS Sanitary ceramic waste Loess	4	22–1150 °C, dwell 4 h	1150	30	Raw material composition	Bloating index; porosity; water absorption; bulk density; crushing strength; SEM; vapour permeability; frost resistance; $CaSO_4$ crystallisation; UV durability; roughness; thermal conductivity; leachability	Andrzejuk et al. (2024)
SS Excavated soil	1 (3 size categories)	Preheat 300 °C	1150	20	Aggregate size	SEM/EDX; loose bulk density; water absorption; crushing strength	Dang et al. (2023)
SS Waste glass powder	1	Heating rate 10 °C min^{-1}	1150–1200	10–60	Sintering temperature Dwell time	Water absorption; particle density; crushing strength; SEM; Micro-CT analysis	Li et al. (2021)
SS Hard clay	6	Preheat 400 °C (10–40 min dwell)	1000–1150	10–40	Raw composition Preheating & sintering time	Particle density; water absorption; bloating index; pore analysis (3D-CT)	Min Wie et al. (2023)
SS Washed aggregate	5	Preheat 300–450 °C (5 min)	1150–1225	10–15	Raw mix Temperature & time	Crushing strength; water absorption; bulk / apparent / dry density; LOI; bloating index	González-Corrochano et al. (2009b)
SS Coal ash	5	Preheat 420 °C (20 min); heating rate 90 °C min^{-1}	1050–1100	30	Composition Temperature	SEM; absorption; density; strength; leachability	Wang et al. (2009a)
SS (only)	1	Preheat 420 °C (20 min); heating rate 90 °C min^{-1}	950–1080	15–45	Temperature Time	Absorption; density; strength; SEM; leachability	Wang et al. (2008)
SS POFA Na_2SiO_3	9	200–800 °C (30 min dwell)	1160–1200	30	Binder Temperature	Particle density; shrinkage index; density; strength; water absorption; microstructure	Lau et al. (2017)
SS Saline clay Smectite	1	Preheat 400–600 °C (30–50 min dwell)	1000–1150	5–20	Preheat Sinter parameters	Strength; density; absorption; shrinkage index; LOI; SEM	Li et al. (2016)
Municipal SS Waste glass powder	5	Heating rate 10 °C min^{-1}	1180	20	Composition	Absorption; density; strength; pore distribution; SEM; XRD; X-ray imaging	Li et al. (2020b)
SS RHA White & red clay	27	Heating rate 8 °C min^{-1}	1100–1250	15	Composition Temperature	LOI; bloating index; absorption; density; strength; SEM	Souza et al. (2020)
SS River sediment	33	200–800 °C (10 min); heating rate 8 °C min^{-1}	1100	30	$K = (Fe_2O_3 + CaO + MgO)/(SiO_2 + Al_2O_3)$; Fe_2O_3:CaO:MgO and SiO_2:Al_2O_3 ratios	Absorption; bulk / particle density; strength; SEM; leachability	Liu et al. (2017)

concluding that the latter exhibited lower densities due to their enhanced gas forming capacity from Fe_2O_3 and unburnt carbon.

The inclusion of binders has been found to increase both bulk and particle densities, while also affecting the shrinkage index of aggregates. Lau et al. (2017) demonstrated that using Na_2SiO_3 as a binder in an SS-POFA mixture increased both bulk and particle densities. This effect arises because Na_2SiO_3 reacts with atmospheric CO_2 to form sodium carbonate, which decomposes during sintering, releasing alkali oxides into the matrix. These oxides lower the eutectic temperature, promote vitrification, and consequently reduce open porosity.

Shrinkage is closely related to the pore structure of aggregates. Ewais et al. (2015) reported that higher shrinkage corresponds to a reduction in pore volume, thereby increasing overall density. Similarly, González-Corrochano et al. (2016) found that bulk and particle densities decrease under the following conditions:

1) Longer pre-sintering dwell time
2) Shorter sintering dwell time
3) Lower sintering temperature

These relationships indicate that extended preheating promotes premature gas release, reducing bloating efficiency, whereas insufficient sintering duration or temperature prevents proper vitrification. Lau et al. (2017) further observed that, in SS-POFA aggregates, particle density increased with rising sintering temperature, as the formation of a viscous glassy phase densified the microstructure. Conversely, Li et al. (2021) reported that for SS-waste glass powder aggregates, particle density decreased with increasing sintering temperature. This contrasting behaviour reflects the sensitivity of density to raw material composition and sintering conditions, as illustrated in Fig. 5(a), which compares loose bulk density variation against sintering temperature from multiple published studies. Raising the temperature from 1150 °C to 1200 °C resulted in a 39.9% reduction in particle density due to excessive bloating and gas release. A similar trend was noted by Latosí Nska et al. (2021) in SS-clay aggregates, where higher sintering temperatures produced lower apparent densities and porosities. This behaviour was attributed to reduced viscosity at elevated temperatures, which inhibits gas entrapment and allows gases to escape, resulting in lower bulk density.

In summary, the density and shrinkage behaviour of sintered SS aggregates are highly sensitive to both material composition and process parameters. Achieving optimal balance between expansion and vitrification is essential for producing aggregates that are lightweight yet mechanically stable.

5.2. Water absorption

The water absorption capacity of sintered aggregates is primarily governed by the formation, size, and connectivity of pores within the material. Aggregates possessing a vitrified and sealed surface, where

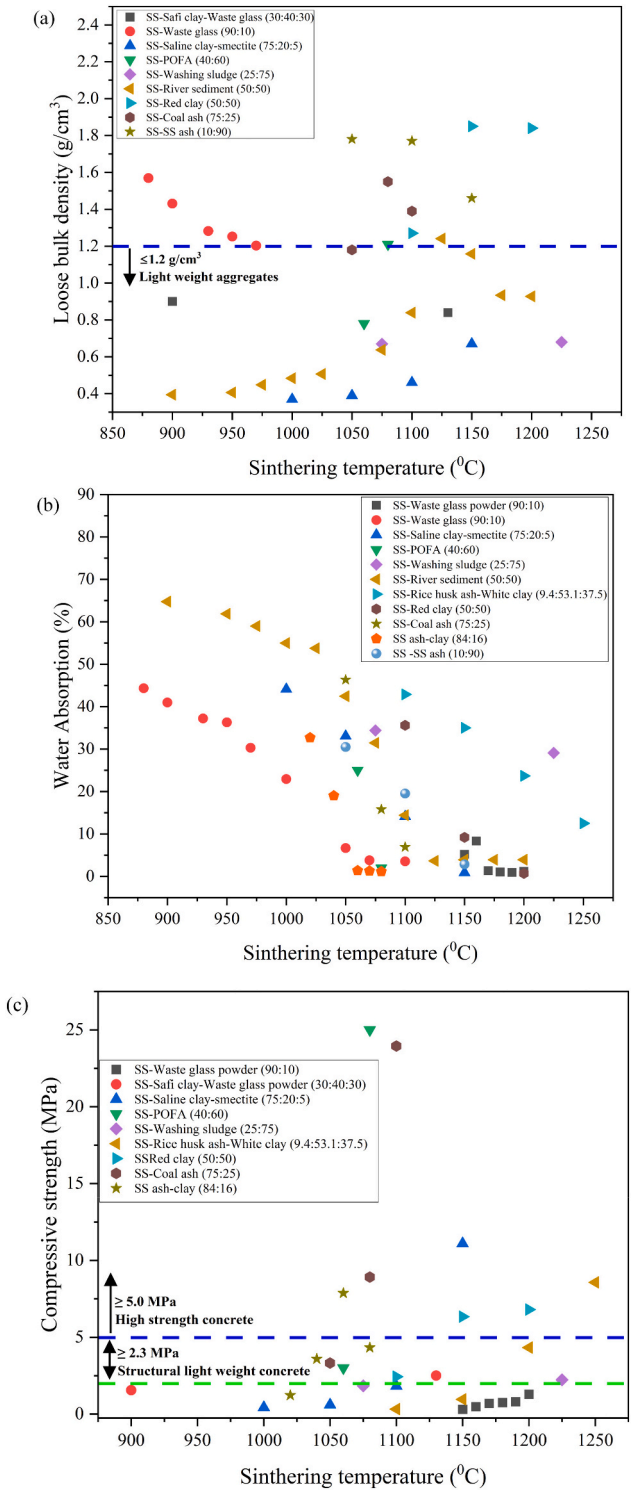

Fig. 5. Effect of sintering temperature on the physical and mechanical properties of sewage sludge based aggregates reported in published studies: (a) loose bulk density variation (Bouachera et al., 2021; Chiou et al., 2006a; González-Corrochano et al., 2016; Lau et al., 2017; Liu et al., 2018b; Souza et al., 2020; Tuan et al., 2013; Wang et al., 2009a); (b) water absorption variation (Bouachera et al., 2021; Cheeseman and Virdi, 2005; Chiou et al., 2006a; González-Corrochano et al., 2016; Li et al., 2016, 2021; Liu et al., 2018b; Souza et al., 2020; Tuan et al., 2013; Wang et al., 2009a); and (c) compressive strength variation (Bouachera et al., 2021; Cheeseman and Virdi, 2005; González-Corrochano et al., 2016; Lau et al., 2017; Li et al., 2016, 2021; Souza et al., 2020; Wang et al., 2009a).

pores are largely isolated, exhibit low water absorption, whereas those with open or interconnected pores demonstrate significantly higher absorption, behaving in a sponge like manner (Lau et al., 2017). When SS is used as the sole raw material in AA production, the resulting matrix often exhibits a highly porous and loosely bound structure, leading to elevated water absorption (Wang et al., 2009a; Xu et al., 2006). This behaviour is attributed to the high organic and moisture content of SS, which increases gas generation during sintering and leaves behind residual porosity. To mitigate this effect, supplementary materials such as clay, coal ash, and fly ash are commonly incorporated to enhance densification and reduce porosity (Liu et al., 2012; Wainwright and Cresswell, 2001; Wang et al., 2009a; Xu et al., 2006). Ren et al. (2021), compared the water absorption characteristics of sintered aggregates derived from SS, clay, and fly ash, finding that SS-based aggregates displayed lower water absorption than fly ash aggregates. This improvement was attributed to the formation of a vitrified surface layer on SS aggregates, which effectively restricted water ingress.

The use of binders further enhances water resistance by reducing the sintering temperature required for glass-phase formation, promoting the development of a dense, impermeable shell (Geetha and Ramamurthy, 2010b; Lau et al., 2017; Ren et al., 2021). In general, increasing the sintering temperature reduces water absorption, as elevated temperatures facilitate particle fusion and surface densification, resulting in fewer open pores (Geng et al., 2024; Li et al., 2021). This overall trend is illustrated in Fig. 5(b), which compiles published data on water absorption variation with sintering temperature for SS-based aggregates. The results demonstrate a clear decline in water absorption as sintering temperature increases, although the exact rate of reduction depends on the raw material composition and binder type. Although water absorption generally decreases with sintering temperature as shown in Fig. 5 (b), it is strongly moderated by mix design (SS fraction, binder chemistry), pellet size distribution, and the thermal profile (preheating, heating rate, dwell time, and cooling regime). Nevertheless, within individual studies where these variables are held constant, water absorption is frequently described by a monotonic decay-type relationship with temperature, which may be represented in generic form as in eq. (1).

$$WA = f(T), \frac{\mathrm{d}(\mathrm{WA})}{\mathrm{dT}} < 0 \tag{1}$$

where WA denotes the water absorption of the sintered aggregate (%) and T represents the sintering temperature (°C). The negative derivative indicates that water absorption decreases as sintering temperature increases, reflecting progressive vitrification, pore closure, and surface densification. It should be noted that Eq. (1) is not intended to represent a universal predictive model, as water absorption is strongly influenced by multiple interacting variables, including raw material composition, flux content, binder type, heating rate, dwell time, and cooling regime. Accordingly, Fig. 5(b) is used to synthesise cross-study trends rather than to derive a global predictive correlation.

Souza et al. (2020) investigated SS-RHA aggregates and reported a consistent reduction in water absorption as the sintering temperature increased from 1100 °C to 1250 °C, across 27 different SS-RHA formulations. A similar trend was observed by Lau et al. (2017) found that in SS-POFA aggregates, raising the sintering temperature from 1160 °C to 1200 °C led to a marked decline in water absorption across nine different mixtures. However, Li et al. (2021) observed a non-linear trend in SS-waste glass powder aggregates, where water absorption initially increased between 1150 °C and 1160 °C, followed by a reduction at 1200 °C. This behaviour was attributed to the competition between gas evolution and vitrification: insufficient viscosity at intermediate temperatures allowed excessive bloating and surface cracking, which were subsequently sealed by vitrification at higher temperatures.

In summary, water absorption in SS-derived aggregates is a function of both microstructural evolution and sintering dynamics. Optimising

temperature, binder type, and additive composition is crucial to achieving a dense, low-permeability matrix. Aggregates exhibiting water absorption below 10% are generally considered suitable for structural lightweight concrete applications, highlighting the potential of SS-based aggregates when processed under controlled sintering conditions.

5.3. Crushing strength

The compressive strength of sintered aggregates is influenced by several interrelated factors, including:

1) The density and shape of the aggregate
2) The pore size distribution and porosity within the matrix
3) The water absorption capacity
4) The softening temperature of the constituent materials
5) The mineralogical composition
6) Densification behaviour during sintering
7) The formation of cracks or internal fractures due to thermal stresses

Several studies (Geng et al., 2024; González-Corrochano et al., 2016; Lau et al., 2017; Li et al., 2021) have reported that the crushing strength of a single sintered aggregate can be determined using eq. (2):

$$S = \frac{2.8P_c}{\pi d^2} \quad (2)$$

where S (MPa) is the single aggregate crushing strength, P_c (N) is the fracture load, and d (mm) is the distance between the upper and lower loading plates. Previous studies (Liao and Huang, 2011; Liu et al., 2018a) recommend a loading rate of 0.1 mm s^{-1} for testing individual aggregate particles.

Liu et al. (2018a) investigated SS-river sediment aggregates and observed a strong correlation between crushing strength and particle density, indicating that strength is largely governed by aggregate porosity. Li et al. (2021) similarly reported that increasing porosity results in lower particle density and reduced strength. However, in SS-waste glass powder aggregates, increasing the sintering temperature from 1160 °C to 1180 °C raised porosity by 13.75%, while crushing strength decreased by only 12.9%. This relatively small reduction was attributed to the transformation of irregular pores into spherical, evenly distributed voids, which distribute stress more uniformly. These findings highlight that pore geometry, rather than porosity alone, plays a critical role in determining crushing strength. Aggregate size is another important factor affecting strength. Several research studies have shown that larger aggregates exhibit lower crushing strength than smaller ones (Gesoğlu et al., 2012; Gomathi and Anandan, 2013; Gomathi and Sivakumar, 2014). Geng et al. (2024) attributed this to the more efficient expulsion of moisture from smaller aggregates during sintering, which leads to a denser microstructure. Baykal and Döven (2000) reported a similar trend, observing that each incremental increase in aggregate diameter resulted in a measurable decrease in crushing strength.

During sintering, the formation of a molten liquid phase contributes positively to strength by producing a vitrified outer shell that enhances mechanical integrity (Ren et al., 2021). Increasing the sintering temperature promotes shrinkage and densification, thereby improving crushing strength. However, excessively high temperatures reduce the viscosity of the molten phase, impeding gas release and potentially causing aggregate collapse (Tang et al., 2023). Moreover, over sintering can cause smaller pores to coalesce into larger ones, weakening the overall structure (Geng et al., 2024). The variation of compressive strength with sintering temperature for different SS-based mixtures is illustrated in Fig. 5(c), which compiles results from several published studies. A general upward trend in strength is observed up to approximately 1150 °C, beyond 1200 °C, a reduction or plateau in strength is commonly observed, attributed to over melting and pore coalescence. Aggregates incorporating supplementary materials such as coal ash, POFA, or waste glass exhibit consistently higher strengths due to their elevated silica and alumina contents, which enhance vitrification and reduce internal defects.

Due to the high organic content of SS, its use at high proportions often leads to excessive gas evolution, inhibiting densification and producing aggregates with lower strength. For example, Lau et al. (2017), reported a crushing strength of only 0.05 MPa for aggregates containing 60% SS in an SS-POFA mix sintered at 1200 °C. Similarly, Souza et al. (2020) recorded 0.4 ± 0.08 MPa for aggregates containing 70% SS in an SS-RHA mix at the same temperature. The incorporation of SiO_2 and Al_2O_3 rich binders, however, can significantly enhance mechanical strength. Lau et al. (2017) observed that adding Na_2SiO_3 to an SS-POFA mix increased crushing strength from 1.5 MPa to 8.1 MPa at 1200 °C. Comparable improvements have been reported in other studies (Souza et al., 2020; Xu et al., 2008, 2006), confirming that silica and alumina based additives promote matrix densification and strengthen the vitrified surface layer.

Table 3 summarises the applicability of AA based on their water absorption and crushing strength. Chen et al. (2010) stated that LWAs with a crushing strength of ≥5 MPa are suitable for the production of Grade 40 concrete. Furthermore, according to the Chinese National Bureau of Standards, a minimum crushing strength of 7.5 MPa is required for LWAs used in civil engineering applications (Liu et al., 2018a).

To contextualize the performance of SS based AAs, it is useful to compare their strength-to-density efficiency with that of commercial LWAs. Past research studies reported that commercial LWAs such as expanded clay, shale, and slate typically exhibit compressive strengths of 5–25 MPa at bulk densities ranging from 300 to 900 kg/m^3, yielding strength-to-density ratios of approximately 0.01–0.04 MPa·m^3/kg (Fořt et al., 2024; Haddadian et al., 2023). In comparison, SS based sintered aggregates frequently achieve crushing or compressive strengths in the range of 5–15 MPa at particle densities between 600 and 1100 kg m^{-3}, resulting in comparable strength-to-density efficiencies. This indicates that, despite their waste derived origin, SS based aggregates can attain mechanical performance efficiencies similar to those of conventional LWAs, particularly when optimised sintering conditions promote controlled bloating and the formation of a vitrified outer shell.

In conclusion, the crushing strength of sintered SS aggregates depends on the delicate balance between bloating and densification. While high gas evolution and porosity reduce strength, controlled sintering and the use of silica rich binders can yield aggregates with both low density and satisfactory mechanical performance for structural use.

5.4. Comparative evaluation of alternative artificial aggregate production routes

While the preceding sections focus on the production and performance of SS derived sintered aggregates, a broader perspective is required to position this approach within the wider landscape of AA

Table 3
LWA classification criteria (Rossignolo, 2009; Souza et al., 2020).

Particle Density (g/cm^3)	Water Absorption (%)	Crush Strength (MPa)	Application
< 2.00	0–20	> 5.00	High-strength concrete
< 2.00	0–20	> 2.30	Structural lightweight concrete
< 2.00	0–34	> 1.80	Non-structural lightweight concrete, Lightweight mortars
< 2.00	10–38	> 1.80	Geotechnical Applications
< 2.00	10–38	> 1.00	Gardening & Landscaping, Thermal and Acoustic Insulation

technologies. AAs can be produced via multiple hardening routes, notably high temperature sintering, cold bonding, and alkali activation, each characterised by distinct processing requirements, energy demands, curing strategies, and performance outcomes (Bekkeri et al., 2023; Lau et al., 2017; Ren et al., 2021; Tian et al., 2021). A comparative evaluation of these routes is therefore essential to assess their relative technological maturity, environmental footprint, and suitability for large scale implementation.

Fig. 6. presents a synthesis of key physical and mechanical properties including water absorption, particle density, loose bulk density, and crushing strength for AAs produced via sintering, cold bonding, and alkali activation, based on data compiled from published literature (Li et al., 2016; Ren et al., 2021; Ruimin et al., 2021; Wainwright and Cresswell, 2001; Wang et al., 2009a). As shown in Fig. 6(a), sintered aggregates generally exhibit lower water absorption compared with cold bonded and alkali activated aggregates. This behaviour is primarily attributed to the formation of a vitrified outer shell during sintering, which effectively inhibits the ingress of water by sealing surface pores.

The particle density trends illustrated in Fig. 6(b) further indicate that sintered aggregates typically possess lower densities than those produced by low temperature routes. This reduction is associated with the bloating phenomenon during sintering, whereby gas evolution at elevated temperatures generates closed internal pores within the aggregate core, thereby reducing overall density (Lau et al., 2017). A similar trend is observed for loose bulk density (Fig. 6(c)). In contrast, cold bonded and alkali activated AAs generally lack significant bloating, and their densities are strongly influenced by the type and dosage of binders used. Many binder systems exhibit relatively high specific gravity and contribute to pore filling, which limits void formation and results in higher aggregate densities (Ren et al., 2021).

Fig. 6(d) compares the crushing strength of aggregates produced via the different processing routes. Alkali activated aggregates frequently demonstrate higher strength development than both sintered and cold bonded counterparts, reflecting the formation of dense reaction products resulting from alkaline activation of aluminosilicate precursors (Ren et al., 2021). However, the strength of aggregates produced by all three routes shows substantial variability, depending on raw material composition, binder chemistry, and curing regime. For example, Ren et al. (2021) reported crushing strengths exceeding 23 MPa for sintered aggregates incorporating bentonite, while similar strength levels have been achieved in alkali activated aggregates formulated with fly ash and GGBS (Gomathi and Sivakumar, 2015; Suresh et al., 2016b).

A critical examination of key process variables, including curing methods, energy intensity, mechanical performance, and environmental safety, is presented in Table 4. to compare the advantages and limitations of the principal AA production routes reported in recent literatures

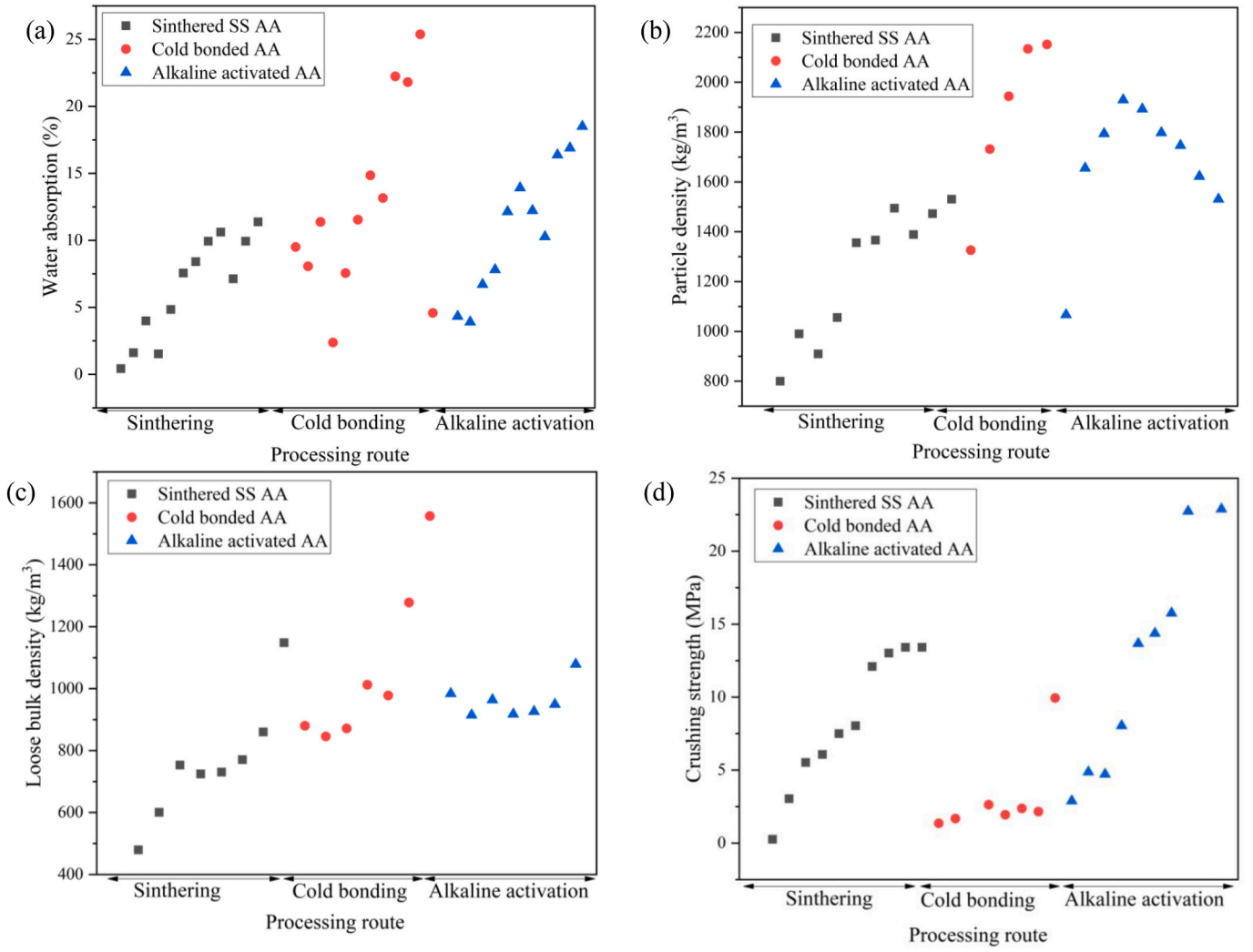

Fig. 6. Literature derived comparison of key physical and mechanical properties of AAs produced via different processing routes: (a) water absorption, (b) particle density, (c) loose bulk density, and (d) crushing strength for sintered, cold-bonded, and alkali-activated aggregates (Li et al., 2016; Ren et al., 2021; Ruimin et al., 2021; Wainwright and Cresswell, 2001; Wang et al., 2009a).

Table 4
Synthesised comparison of sintering, cold bonding, and alkali activated AA production routes based on representative studies reported in the recent literature (Andrzejuk et al., 2024; Bekkeri et al., 2023; Duan et al., 2025; Geetha and Ramamurthy, 2010b; Geng et al., 2024; Gesoğlu et al., 2012; Gomathi and Sivakumar, 2014; Ren et al., 2021; Wainwright and Cresswell, 2001; Wang et al., 2009b, 2008; Yang et al., 2023).

Criterion	Sintering based aggregates	Cold bonded aggregates	Alkali activated aggregates
Primary hardening mechanism	Thermal expansion (bloating) coupled with vitrification at elevated temperatures, producing a porous core and dense outer shell	Hydraulic hydration and pozzolanic reactions forming a cementitious binding matrix	Chemical geopolymerisation via alkaline dissolution and re-polymerisation of aluminosilicates
Typical temperature regime	High temperature (>1000–1200 °C)	Ambient to low temperature (≤60 °C)	Ambient to moderately elevated temperature (≤80 °C)
Key raw materials	SS, clay, shale, fly ash, industrial residues	SS ash, fly ash, slag, quarry fines, recycled powders	SS ash, fly ash, slag, metakaolin, aluminosilicate rich wastes
Binder/activator system	Self fluxing oxides inherent to feedstock composition	Cement, lime, blended mineral binders	NaOH, Na_2SiO_3, or combined alkaline activators
Pelletisation step	Disc or drum pelletisation	Disc or drum pelletisation	Disc or drum pelletisation
Curing / hardening strategies	Preheating Rotary kiln sintering Controlled cooling	Natural curing (ambient) Oven curing Steam curing Carbonation curing Autoclave curing	Ambient curing Mild thermal curing Steam curing Autoclave curing
Typical curing / processing time	Minutes to hours	Days to weeks (curing method dependent)	Hours to days (curing method dependent)
Energy demand	Very high due to thermal sintering	Low (dominated by binder production)	Low-moderate (dominated by activator production and curing)
CO_2 emission profile	High (fuel combustion and process emissions)	Low to moderate (cement content dependent)	Low to moderate (activator manufacturing dependent)
Bulk density (typical range)	Low (800–1200 kg m^{-3})	Moderate (900–1600 kg m^{-3})	Moderate (900–1400 kg m^{-3})
Crushing strength	Moderate to high (>6–10 MPa)	Moderate (~3–8 MPa), highly mix-dependent	Generally high (~6–17 MPa) with optimised curing
Water absorption behaviour	Low to moderate due to vitrified shell and isolated pores	Often high due to open pore networks unless surface densification is applied	Typically, lower than conventional cold bonding owing to denser reacted shell
Heavy metal immobilisation	Excellent Encapsulation within vitrified/crystalline matrix	Moderate Strongly dependent on binder chemistry	Good Chemical binding and encapsulation, element-specific behaviour
Process complexity	High (kilns, fuel supply, emission control)	Low (simple equipment and ambient curing)	Moderate (alkali handling, curing control)
Technological maturity	Industrially established	Pilot to early industrial scale	Predominantly laboratory to pilot scale
Key advantages	High strength Durability Low absorption Robust environmental safety	Low energy demand Simple processing Strong circular-economy potential	Cement-free binding Improved performance over cold bonding Reduced thermal demand
Key limitations	High energy consumption High CAPEX/OPEX Greenhouse gas emissions	Long curing times Higher absorption Performance variability	Alkali cost and safety concerns Durability and standardisation gaps
Critical improvement needs	Lower temperature sintering Energy recovery Emission reduction strategies	Rapid curing methods Cement free binders Pore sealing and durability enhancement	Optimised activator systems Safer handling protocols Long-term durability validation

(Andrzejuk et al., 2024; Bekkeri et al., 2023; Duan et al., 2025; Geetha and Ramamurthy, 2010b; Geng et al., 2024; Gesoğlu et al., 2012; Gomathi and Sivakumar, 2014; Wainwright and Cresswell, 2001; Wang et al., 2009b, 2008; Yang et al., 2023). Particular emphasis is placed on curing regimes for cold bonded and alkali activated aggregates, as these strongly influence strength development, durability, and scalability. This comparative analysis provides context for SS based sintering while highlighting alternative low temperature pathways and identifying key areas where further optimisation and standardisation are required.

Although most studies on SS based AAs are conducted at laboratory scale, several aspects of the proposed production routes are compatible with existing industrial practice. In particular, sintering based production can be directly aligned with established rotary kiln technologies currently used for LWA manufacture, suggesting clear potential for scale up. From a techno economic perspective, thermal energy demand remains the dominant cost and emission contributor (Yang et al., 2023). However, this may be partially offset by the high organic content of SS, which can act as an internal fuel, as well as by avoided sludge disposal and natural aggregate extraction costs(Mohanta and Murmu, 2022; Peduzzi and Peduzzi, 2014; Yang et al., 2023). Low-temperature routes such as cold bonding and alkali activation offer advantages in reduced energy demand, but challenges related to curing time, binder or activator cost, and performance consistency at larger scales remain (Ren et al., 2021; Tang et al., 2020). Overall, wider adoption will depend on pilot-scale validation, regulatory acceptance, and the development of standardised performance criteria for waste-derived aggregates.

5.5. *Environmental safety of sewage sludge-based aggregates: Heavy metals and organic contaminants*

SS contains potentially harmful heavy metals such as chromium (Cr), cadmium (Cd), copper (Cu), molybdenum (Mo), antimony (Sb), zinc (Zn), lead (Pb), nickel (Ni), and selenium (Se), which can leach into the environment and pose serious ecological and human health risks (Donatello et al., 2010; Li and Zhang, 2021; Sidhu et al., 2024). Among these, Pb exposure has been associated with neurotoxicity and developmental impairment, underscoring the importance of controlling contaminant release during the production and application of SS-based AAs (Wang et al., 2020).

Table 5 summarises the leachate limit values for key heavy metals according to the European Landfill Waste Acceptance Criteria (WAC) guidelines (CEN, 2002) and contextualises their relevance to SS-based aggregate production. Experimental studies consistently demonstrate that sintering significantly reduces the leachability of most heavy

Table 5
Leachate limits specified by European Landfill Waste acceptance criteria guidelines (CEN, 2002; EN, B.S, 2002; Sidhu et al., 2024; Wang et al., 2020).

Element	Inert waste limit (mg L^{-1})	Non-hazardous waste limit (mg L^{-1})	Hazardous waste limit (mg L^{-1})	Environmental relevance	Implications for SS based AA
Cu	2.0	50	100	Toxic to aquatic organisms at elevated concentrations	Typically immobilised in vitrified or cementitious matrices
Zn	4.0	50	70	Mobile in acidic conditions Phytotoxic	Generally stabilised during high-temperature sintering
Pb	0.5	10	50	Neurotoxic Strict regulatory control	Effectively encapsulated in glassy phases
Cd	0.04	1.0	5.0	Highly toxic even at low concentrations	Strongly immobilised via vitrification and mineral bonding
Ni	0.4	10	40	Potential carcinogen Groundwater concern	Partial stabilisation; sensitive to pH conditions
Se	0.1	0.5	7.0	Bio accumulative Ecosystem toxicity	Generally low leachability after sintering
As	0.5	2.0	25	Carcinogenic Redox-sensitive	Immobilisation depends on oxidation state and matrix
Cr	0.5	10	70	Cr(VI) highly toxic and mobile	Reduced leaching through high temperature treatment
Ba	20	100	300	Groundwater contamination risk	Typically remains within inert limits
Mo	0.5	10	30	High mobility in alkaline systems	May require optimisation of matrix chemistry
Hg	0.01	0.2	2.0	Volatile and highly toxic	Effectively retained in vitrified structures
Sb	0.06	0.7	5.0	Emerging contaminant Increasing regulation	Generally low release in SS-based AAs

metals. For example, Franus et al. (2016) reported that SS-clay aggregates containing 10 wt% SS exhibited metal concentrations well below regulatory limits, attributed to immobilisation within aluminosilicate mineral lattices such as beidellite, illite, and kaolinite. Similarly, Geng et al. (2024) observed that although Zn leaching from sintered aggregates was marginally higher than that from green granules, all values remained compliant with regulatory thresholds.

Sintering temperature plays a decisive role in heavy metal stabilisation. Liu et al. (2018a) showed that increasing the sintering temperature from 950 °C to 1050 °C markedly enhanced the immobilisation of Cd, Cr, Cu, and Pb, owing to the formation of a continuous liquid phase that encapsulates metals within a vitrified matrix. At lower temperatures, incomplete vitrification limits stabilisation efficiency. Comparable trends were reported by Wang et al. (2008) who noted reduced leaching of As, Cd, and Cr at higher firing temperatures, although Ni, Pb, and Zn showed more limited sensitivity. These findings indicate that the effectiveness of immobilisation depends on elemental properties such as volatility, ionic radius, and bonding affinity within the glassy or crystalline phases.

In addition to inorganic contaminants, SS is known to contain harmful organic pollutants, notably PFAS, pharmaceuticals, and personal care products. Table 6 provides an integrated assessment of PFAS occurrence in SS and biosolids, associated regulatory thresholds, partitioning behaviour, and reported thermal treatment effectiveness. Reported PFAS concentrations in SS often approach or exceed regulatory limits for land application, highlighting the need for destructive or immobilising treatment prior to reuse.

Unlike land-application scenarios, the high-temperature sintering process employed for SS-based aggregate production typically exceeds 1000–1200 °C, well above the thermal degradation thresholds reported for most PFAS compounds. Literature consistently indicates near complete destruction of PFAS at temperatures above 700–800 °C, particularly when coupled with oxidative conditions that prevent secondary emissions (Arvaniti et al., 2012; Ismail and Tizaoui, 2025; Schlederer et al., 2024; Winchell et al., 2024). Consequently, sintered SS-based aggregates present a substantially lower risk associated with organic contaminants compared with untreated or low-temperature-treated sludge.

Overall, the combined effects of vitrification, mineral encapsulation, and high-temperature degradation render sintering a technically robust and environmentally sound route for mitigating both inorganic and organic contaminant risks in SS-based aggregates. While available evidence strongly supports compliance with EU WAC limits, further systematic leachate and durability testing under long-term service conditions would strengthen regulatory confidence and facilitate broader industrial adoption.

6. Sustainability assessment of sewage sludge-based aggregates

6.1. Socio economic and sustainability implications of sewage sludge-based aggregates

The global construction industry faces mounting challenges due to the diminishing availability of conventional aggregates. According to the United Nations Environment Programme (UNEP), annual aggregate consumption is approximately 50 billion tonnes, and demand is projected to rise in parallel with global economic and population growth (OECD, 2019). Given the finite nature of natural aggregate resources, meeting this escalating demand represents a critical long-term challenge for the construction sector (Lau et al., 2017).

The forecasted demand for concrete infrastructure, gravel, and stone, together with predictions of known gravel resource availability, are presented in the Supplementary Information (Fig. S2). These data indicate that demand for gravel, stone, and concrete infrastructure continues to increase, particularly for road construction, paving, and structural applications. However, this trajectory directly conflicts with the declining availability of gravel reserves and rising concerns regarding the environmental and social impacts of extraction. Efforts to sustain supply rely on the identification of new reserves, the granting of extraction permits, and the rehabilitation of depleted sites (Bendixen et al., 2021a). Yet, replenishment rates fall well below consumption. The Mineral Products Association (2017) reports that only 61% of land-won sand and gravel is currently replaced through new planning permissions, indicating a trajectory of resource depletion incompatible with long-term sectoral growth.

The socio-economic implications extend beyond resource scarcity. Aggregate mining has become a subject of public and media scrutiny, often framed through the lens of illegality and informal operations the so-called “sand mafia” phenomenon (Bisht and Gerber, 2017; Mahadevan, 2019). While this framing draws attention to governance failures, it oversimplifies a complex global issue. In many developing regions, informal sand and gravel extraction provides a crucial livelihood for impoverished communities. Conversely, there is abundant evidence linking unregulated aggregate mining to ecological degradation,

Table 6
Integrated assessment of PFAS occurrence, regulatory thresholds, partitioning behaviour, and thermal treatment effectiveness in sewage sludge and biosolids.

Aspect	Key findings (quantitative)	Implications for sewage sludge based artificial aggregates	Ref
PFAS concentration in sewage sludge and biosolids	PFOS: <0.01–552.6 ng/g dw PFOA: <0.01–601 ng/g dw PFHxS: <0.01–157.7 ng/g d PFBS: <0.01–36.97 ng/g dw (region- and treatment-dependent)	Confirms sewage sludge as a significant reservoir of long chain PFAS, necessitating robust treatment prior to valorisation	(Bossi et al., 2008; Letcher et al., 2020; Moodie et al., 2021; Stahl et al., 2018; Venkatesan and Halden, 2013; Zhou et al., 2024)
Regulatory thresholds (soil/sludge)	PFOS limits: 1–390 ng/g dw (EU, Australia, USA) PFOS+PFOA: 100 ng/g dw (Germany, Austria) PFBS up to 1900 ng/g dw (Canada)	Many reported sludges concentrations approach or exceed regulatory limits, underscoring the need for destructive or immobilising treatments	(Government, 2016; Hall, 2021; Zhou et al., 2024)
PFAS partitioning in sludge (log Kd, L/kg)	Long-chain PFAS show strong sorption 1. PFOS ~2.6–4.0 2. PFUnDA ~3.5–3.9 3. PFDA ~3.0–3.7 Short chain PFAS show weaker sorption (~0.6–1.5)	Strong sorption implies persistence in solids Physical separation alone is insufficient thermal or chemical transformation required	(Arvaniti et al., 2012; Ismail and Tizaoui, 2025; Lewis et al., 2023)
Low-temperature thermal treatment (<400 °C)	Incomplete PFAS removal Redistribution to biochar Py-oil or gas phases frequently observed	Unsuitable as a stand alone mitigation strategy for SS valorisation into construction products	(Hušek et al., 2024)
Intermediate-temperature thermal treatment (500–700 °C)	Significant PFAS reduction Partial transfer to gas/oil unless secondary treatment applied	Indicates temperature sensitivity of PFAS degradation Process integration required	(Ismail and Tizaoui, 2025; McNamara et al., 2022; Sørmo et al., 2023)
High-temperature thermal treatment (>700–800 °C)	Near complete PFAS destruction residual PFAS often below detection limits	Confirms thermal severity threshold for effective PFAS elimination	(Schlederer et al., 2024; Sørmo et al., 2023)
Thermal treatment with oxidation coupling	Pyrolysis + thermal oxidation achieves PFAS concentrations below detection in solids and scrubber water.	Demonstrates importance of gas phase treatment to prevent secondary emissions	(Ismail and Tizaoui, 2025)
Relevance to sintered SS-based aggregates	Sintering temperatures typically >1000–1200 °C, exceeding PFAS destruction thresholds reported in all studies	Strong evidence that SS based sintered aggregates provide superior PFAS mitigation compared with low temperature routes	(Hušek et al., 2024; Winchell et al., 2024)
Environmental risk mitigation pathway	High-temperature vitrification encapsulates residual inorganic contaminants while destroying organics	Supports environmental safety of SS derived aggregates within EU waste acceptance criteria	(Ren et al., 2021; Zhou et al., 2024)

landscape disruption, and labour rights violations (Bisht, 2021). Hence, aggregate extraction embodies a dual socio-economic reality: it sustains livelihoods while simultaneously exacerbating environmental and social vulnerabilities.

Dredging and large-scale mining operations also leave visible scars on the landscape, and urgent measures are required to safeguard biodiversity from both direct habitat loss and indirect geomorphological impacts, such as altered sedimentation in rivers, floodplains, and coastal ecosystems (Bendixen et al., 2021a). Historically, these impacts were not considered major threats to aquatic biodiversity, and few protected areas were established to mitigate mining pressures. The growing body of evidence highlighting the adverse ecological consequences of aggregate extraction, coupled with the limited conservation response, poses a serious risk to global biodiversity, particularly concerning SDGs 14 (Life Below Water) and 15 (Life on Land) (Bendixen et al., 2021a; Cicin-Sain and Belfiore, 2005; Saunders et al., 2002). Furthermore, the construction and building sectors collectively account for approximately 39% of global energy-related CO_2 emissions. Promoting circular economy initiatives, such as the utilisation of SS in aggregate production, offers a pathway to reduce dependence on virgin raw materials, minimise carbon emissions, and directly support climate change mitigation efforts (SDG 13: Climate Action) (Dagnachew and Hof, 2022).

With an annual generation of approximately 53 million tonnes, SS represents a substantial secondary resource capable of partially or even fully substituting natural aggregates in both structural and non-structural applications (Bendixen et al., 2021a). The adoption of SS-based aggregates can thus generate economic, environmental, and social co-benefits:

1. Economic, through reduced raw-material costs and waste-management expenditures.
2. Environmental, through resource conservation and lower greenhouse-gas emissions
3. Social, through the creation of green jobs and the promotion of sustainable construction practices

By integrating SS into the aggregate supply chain, the construction sector can transition toward a more resilient and circular economic model, balancing material efficiency with social equity and environmental stewardship.

6.2. *Comparative life cycle energy, carbon and cost performance of sewage sludge-based aggregates*

A quantitative evaluation of CO_2 emissions, energy consumption, and production cost provides a clearer basis for assessing the suitability of SS based AA as an alternative to natural aggregates in the construction industry. To enable a consistent comparison, life-cycle assessment (LCA) based data reported in the published literature were compiled and synthesised, with particular emphasis on studies providing detailed inventories of fuel consumption, electricity use, and transportation requirements (Piippo et al., 2018; Yang et al., 2023). It should be noted that no new experimental data were generated; rather, the present analysis builds upon primary data reported in existing peer-reviewed studies, notably the comprehensive LCA framework proposed by Yang

et al. (2023).

For SS based AAs, the main processing stages typically include sludge drying, transportation, compaction and moulding, drying of green pellets, and high-temperature sintering, whereas natural aggregates production involves drilling, excavation, crushing, screening, and transportation (Bendixen et al., 2021b; Lau et al., 2017; Mahadevan, 2019; Peduzzi and Peduzzi, 2014). For comparison purposes, a functional unit of 1 t of aggregate was adopted for both systems. Published data on fuel consumption for transport, natural gas usage for sintering, and electricity demand for auxiliary operations were collected and normalised to this functional unit (Yang et al., 2023).

Transportation related CO_2 emissions were calculated using the approach reported by Yang et al. (2023) and D. Li et al. (2020), expressed as in eq. (3):

$$CO_2\ emission = \Sigma_i\left(\left(E_{i,l} + E_{i,e}\right)\ x\ \Sigma_{n=1}^{n} m_n x d_n^i\right) \quad (3)$$

Where i denotes the transport mode, $E_{i,l}$ and $E_{i,e}$ are the emission factors for loaded and empty vehicles, respectively, n denotes the type of materials and m_n and d_n^i represent the mass of material and transport distance. Emissions associated with sludge drying and thermal processing were estimated based on reported fossil fuel consumption by Yang et al. (2023), using standard emission coefficients according to eq. (4):

$$CO_2\ emission\ (kg) = Fuel\ used\ x\ Energy\ content\ x\ CO_2\ emssion\ factor \quad (4)$$

The resulting stage-wise CO_2 emissions for SS based AAs and natural aggregates are presented in Fig. 7(a). The total CO_2 emissions were estimated as 441 kg CO_2 tonne^{-1} for SS based AAs and 604 kg CO_2 tonne^{-1} for natural aggregates, indicating that SS based AAs exhibit an approximately 27% lower global warming potential. This reduction is primarily attributed to lower transportation-related emissions and waste valorisation benefits, despite the energy-intensive sintering step.

Energy consumption and associated costs were subsequently evaluated using energy demand values reported by Yang et al. (2023), combined with scenario-based unit energy prices representative of 2025 market conditions. The assumed costs were £0.06 kWh^{-1} for thermal energy (sintering), £0.15 kWh^{-1} for transport (diesel), and £0.28 kWh^{-1} for electricity and auxiliary processes. The resulting energy demand and cost breakdowns are illustrated in Fig. 7 (b and c).

The total energy demand was estimated as 1875 kWh tonne^{-1} for SS based AAs and 1569 kWh tonne^{-1} for natural aggregates. While sintering dominates the energy demand for SS based AAs, transportation constitutes the principal energy contributor for natural aggregates. Importantly, the total production cost derived from this energy cost proxy was £280.10 t^{-1} for SS based AAs compared with £436.96 t^{-1} for natural aggregates, indicating that SS based aggregates are approximately 36% cheaper under the assumed conditions. This cost advantage is largely driven by substantially lower transportation energy demand.

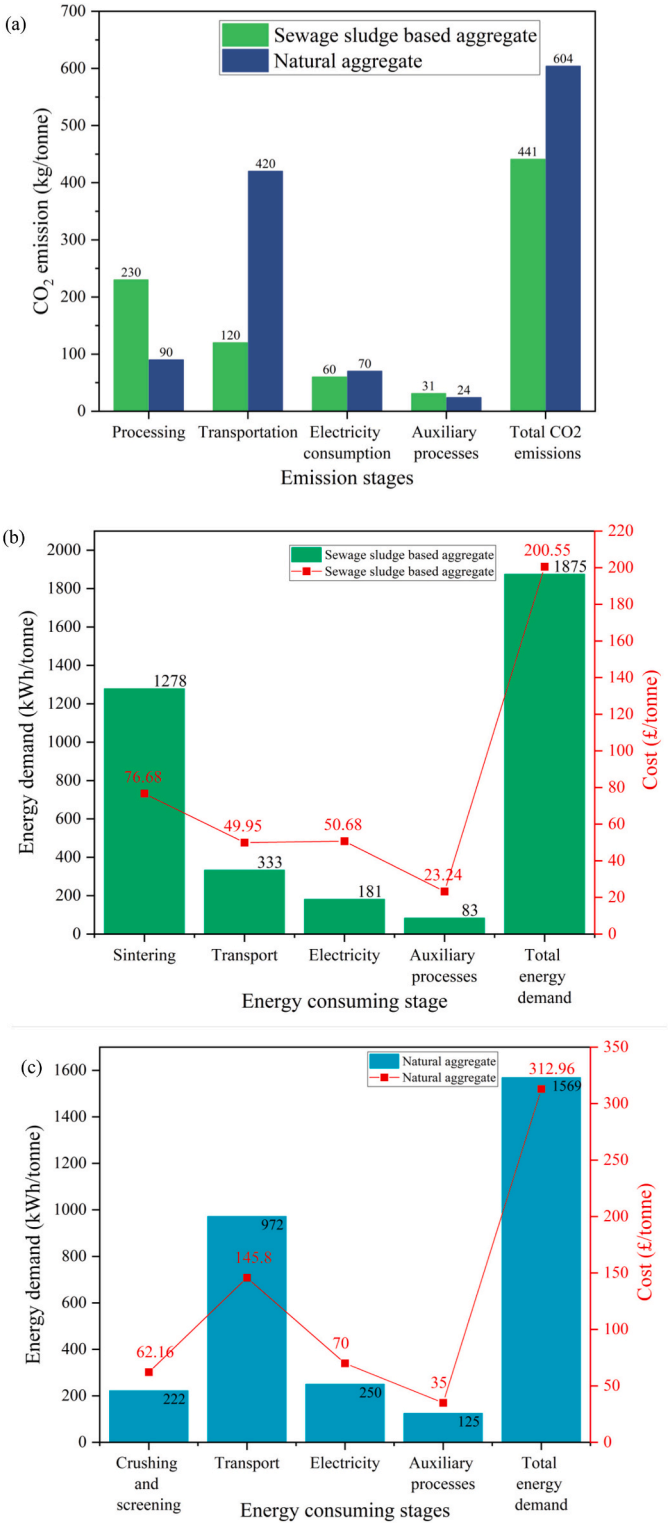

Fig. 7. Stage wise comparison of life cycle CO_2 emissions (kg CO_2 tonne^{-1}), energy demand (kWh tonne^{-1}), and associated production costs (£ tonne^{-1}) for sewage sludge based artificial aggregates and natural aggregates: (a) CO_2 emissions; (b) energy demand and cost for Sewage sludge based artificial aggregates; (c) energy demand and cost for natural aggregates.

7. Conclusion

This review synthesised the current state of knowledge on the valorisation of SS into AAs, with emphasis on processing mechanisms, performance characteristics, environmental safety, and economic implications. The analysis demonstrates that SS exhibits intrinsic suitability for LWA production, as its organic content and mineral composition promote gas evolution, bloating, and vitrification during sintering, enabling strength to density efficiencies comparable to commercial LWAs when appropriately optimised. Sintering temperature and raw material blending were identified as the dominant parameters governing aggregate performance, with optimal properties consistently reported within a relatively narrow temperature range (approximately 1050–1200 °C). High temperature sintering also provides robust environmental risk mitigation by immobilising heavy metals within vitrified matrices and effectively reducing organic contaminant risks, including PFAS, thereby ensuring compliance with regulatory acceptance criteria. Life cycle assessments reported in the literature indicate that SS based aggregates can achieve lower global warming potential and competitive

production costs relative to natural aggregates, largely due to reduced transportation requirements and the valorisation of an unavoidable wastewater by product. While alternative low temperature routes such as cold bonding and alkali activation offer energy saving potential, their current variability in mechanical performance and durability highlights the need for further optimisation. Overall, SS valorisation into AAs represents a viable pathway toward resource efficiency, waste reduction, and circular bioeconomy implementation, strongly aligning with the objectives of UN SDGs 6, 12, and 13.

CRediT authorship contribution statement

Kannan Thushanthan: Writing – review & editing, Writing – original draft, Visualization, Validation, Methodology, Investigation, Formal analysis, Data curation, Conceptualization. **Muhammad Abdul Mannan:** Writing – review & editing, Supervision, Resources, Investigation, Data curation, Conceptualization. **Muhammad Ekhlasur Rahman:** Writing – review & editing, Supervision, Project administration, Funding acquisition, Conceptualization. **Keerthan Poologanathan:** Writing – review & editing. **Mujib Rahman:** Writing – review & editing, Resources, Conceptualization.

Declaration of competing interest

The authors declare that they have no known competing financial interests or personal relationships that could have appeared to influence the work reported in this paper.

Acknowledgements

The authors gratefully acknowledge the financial support provided by Northumbrian Water Group, United Kingdom. The authors are grateful for the support provided by Northumbria University, Newcastle upon Tyne, England. The authors gratefully acknowledge the valuable support provided by Dr. Ulugbek Azimov, Northumbria University.

Appendix A. Supplementary data

Supplementary data to this article can be found online at https://doi.org/10.1016/j.biteb.2026.102658.

Data availability

No data was used for the research described in the article.

References

A, E.P, 1994. A plain English Guide to the EPA Part 503 Biosolids Rule. EPA.
Ábrego, J., Arauzo, J.S., Sánchez, J.L., Gonzalo, A., Cordero, T., Rodríguez-Mirasol, J., 2009. Structural changes of sewage sludge char during fixed-bed pyrolysis. In: Ind. Eng. Chem. Res., 48, pp. 3211–3221. https://doi.org/10.1021/IE801366T/ASSET/IMAGES/LARGE/IE-2008-01366T_0013.JPEG.
Adell, V., Cheeseman, C.R., Ferraris, M., Salvo, M., Smeacetto, F., Boccaccini, A.R., 2007. Characterising the sintering behaviour of pulverised fuel ash using heating stage microscopy. Mater. Charact. 58, 980–988. https://doi.org/10.1016/J.MATCHAR.2006.10.004.
Andrzejuk, W., Grzegorczyk-Frańczak, M., Barnat-Hunek, D., Franus, M., Łagód, G., 2024. Microstructure, durability and surface free energy of lightweight aggregate modification of sanitary ceramic wastes and sewage sludge. J. Build. Eng. 93, 109725. https://doi.org/10.1016/j.jobe.2024.109725.
Arslan, H., Baykal, G., 2006. Utilization of fly ash as engineering pellet aggregates. Environ. Geol. 50, 761–770. https://doi.org/10.1007/s00254-006-0248-7.
Arvaniti, O.S., Ventouri, E.I., Stasinakis, A.S., Thomaidis, N.S., 2012. Occurrence of different classes of perfluorinated compounds in Greek wastewater treatment plants and determination of their solid-water distribution coefficients. J. Hazard. Mater. 239–240, 24–31. https://doi.org/10.1016/j.jhazmat.2012.02.015.
Aubain, P., Gazzo, A., Moux, J., Le, 2002. Disposal and Recycling Routes for Sewage Sludge-Synthesis Report.
Bagheri, M., Bauer, T., Burgman, L.E., Wetterlund, E., 2023. Fifty years of sewage sludge management research: Mapping researchers' motivations and concerns. J. Environ. Manag. 325, 116412. https://doi.org/10.1016/j.jenvman.2022.116412.
Baykal, G., Döven, A.G., 2000. Utilization of fly ash by pelletization process; theory, application areas and research results. Resour. Conserv. Recycl. 30, 59–77. https://doi.org/10.1016/S0921-3449(00)00042-2.
Bekkeri, G.B., Shetty, K.K., Nayak, G., 2023. Synthesis of artificial aggregates and their impact on performance of concrete: a review. J Mater Cycles Waste Manag 25, 1988–2011. https://doi.org/10.1007/s10163-023-01713-9.
Bendixen, M., Iversen, L.L., Best, J., Franks, D.M., Hackney, C.R., Latrubesse, E.M., Tusting, L.S., 2021a. Sand, gravel, and UN sustainable development goals: conflicts, synergies, and pathways forward. One Earth 4, 1095–1111. https://doi.org/10.1016/J.ONEEAR.2021.07.008/ASSET/AAD3E8F4-44C6-4BB0-AAE2-10E79827C2FD/MAIN.ASSETS/FX5.JPG.
Bendixen, M., Iversen, L.L., Best, J., Franks, D.M., Hackney, C.R., Latrubesse, E.M., Tusting, L.S., 2021b. Sand, gravel, and UN Sustainable Development Goals: Conflicts, synergies, and pathways forward. One Earth 4, 1095–1111. https://doi.org/10.1016/J.ONEEAR.2021.07.008.
Bianchini, A., Bonfiglioli, L., Pellegrini, M., Saccani, C., 2016. Sewage sludge management in Europe: a critical analysis of data quality. Int. J. Environ. Waste Manag. 18, 226–238. https://doi.org/10.1504/IJEWM.2016.080795.
Bisht, A., 2021. Conceptualizing sand extractivism: Deconstructing an emerging resource frontier. Extr Ind Soc 8, 100904. https://doi.org/10.1016/J.EXIS.2021.100904.
Bisht, A., Gerber, J.F., 2017. Ecological distribution conflicts (EDCs) over mineral extraction in India: an overview. Extr Ind Soc 4, 548–563. https://doi.org/10.1016/J.EXIS.2017.03.008.
Bossi, R., Strand, J., Sortkjær, O., Larsen, M.M., 2008. Perfluoroalkyl compounds in Danish wastewater treatment plants and aquatic environments. Environ. Int. 34, 443–450. https://doi.org/10.1016/j.envint.2007.10.002.
Bouachera, R., Kasimi, R., Ibnoussina, M., Hakkou, R., Taha, Y., 2021. Reuse of sewage sludge and waste glass in the production of lightweight aggregates. Mater. Today Proc. 37, 3866–3870. https://doi.org/10.1016/J.MATPR.2020.08.410.
BS EN 13055–1, 2002. Lightweight aggregates - Lightweight aggregates for concrete, mortar and grout.
Buta, M., Hubeny, J., Zieliński, W., Harnisz, M., Korzeniewska, E., 2021. Sewage sludge in agriculture – the effects of selected chemical pollutants and emerging genetic resistance determinants on the quality of soil and crops – a review. Ecotoxicol. Environ. Saf. 214, 112070. https://doi.org/10.1016/J.ECOENV.2021.112070.
Capodaglio, A.G., Callegari, A., 2023. Energy and resources recovery from excess sewage sludge: a holistic analysis of opportunities and strategies. Resources, Conservation & Recycling Advances 19, 200184. https://doi.org/10.1016/J.RCRADV.2023.200184.
CEN, 2002. Characterisation of Waste : Leaching : Compliance Test for Leaching of Granular Waste Materials and Sludges. Part 2, One Stage Batch Test at a Liquid to Solid Ratio of 10 L/Kg for Materials with Particle Size below 4 Mm (without or with Size Reduction). British Standards Institution.
Chagas, J.K.M., Figueiredo, C.C., de, da Silva, J., Paz-Ferreiro, J., 2021. The residual effect of sewage sludge biochar on soil availability and bioaccumulation of heavy metals: evidence from a three-year field experiment. J. Environ. Manag. 279, 111824. https://doi.org/10.1016/j.jenvman.2020.111824.
Cheeseman, C.R., Virdi, G.S., 2005. Properties and microstructure of lightweight aggregate produced from sintered sewage sludge ash. Resour. Conserv. Recycl. 45, 18–30. https://doi.org/10.1016/J.RESCONREC.2004.12.006.
Chen, H.J., Wang, S.Y., Tang, C.W., 2010. Reuse of incineration fly ashes and reaction ashes for manufacturing lightweight aggregate. Constr. Build. Mater. 24, 46–55. https://doi.org/10.1016/J.CONBUILDMAT.2009.08.008.
Chen, Q., Zhang, L., Liu, X., Ji, X., Wang, X., Wang, H., Li, A., 2024. Sewage sludge enhances cold-pressed pelletization and carbothermic reduction of steel plant sintering dust. J. Clean. Prod. 463, 142689. https://doi.org/10.1016/j.jclepro.2024.142689.
Chiou, I.J., Wang, K.S., Chen, C.H., Lin, Y.T., 2006. Lightweight aggregate made from sewage sludge and incinerated ash. Waste Manag. 26, 1453–1461. https://doi.org/10.1016/J.WASMAN.2005.11.024.
Cicin-Sain, B., Belfiore, S., 2005. Linking marine protected areas to integrated coastal and ocean management: a review of theory and practice. Ocean Coast. Manag. 48, 847–868. https://doi.org/10.1016/J.OCECOAMAN.2006.01.001.
Colangelo, F., Messina, F., Cioffi, R., 2015. Recycling of MSWI fly ash by means of cementitious double step cold bonding pelletization: Technological assessment for the production of lightweight artificial aggregates. J. Hazard. Mater. 299, 181–191. https://doi.org/10.1016/J.JHAZMAT.2015.06.018.
Collivignarelli, M.C., Abbà, A., Castagnola, F., Bertanza, G., 2017. Minimization of municipal sewage sludge by means of a thermophilic membrane bioreactor with intermittent aeration. J. Clean. Prod. 143, 369–376. https://doi.org/10.1016/J.JCLEPRO.2016.12.101.
Collivignarelli, M.C., Canato, M., Abbà, A., Carnevale Miino, M., 2019. Biosolids: what are the different types of reuse? J. Clean. Prod. 238, 117844. https://doi.org/10.1016/j.jclepro.2019.117844.
Council of the European Communities, 1986. Sewage Sludge Directive (86/278/EEC). Official Journal of the European Union (Off. J. Eur. Union) 4, 6–12.
Dagnachew, A.G., Hof, A.F., 2022. Climate change mitigation and SDGs: modelling the regional potential of promising mitigation measures and assessing their impact on other SDGs. J. Integr. Environ. Sci. 19, 289–314. https://doi.org/10.1080/1943815X.2022.2146137.

Dang, J., Hao, L., Xiao, J., Ding, T., 2023. Utilization of excavated soil and sewage sludge for green lightweight aggregate and evaluation of its influence on concrete properties. J. Clean. Prod. 390, 136061. https://doi.org/10.1016/j.jclepro.2023.136061.

de' Gennaro, R., Cappelletti, P., Cerri, G., de' Gennaro, M., Dondi, M., Langella, A., 2004. Zeolitic tuffs as raw materials for lightweight aggregates. Appl. Clay Sci. 25, 71–81. https://doi.org/10.1016/J.CLAY.2003.08.005.

Donatello, S., Tyrer, M., Cheeseman, C.R., 2010. EU landfill waste acceptance criteria and EU hazardous Waste Directive compliance testing of incinerated sewage sludge ash. Waste Manag. 30, 63–71. https://doi.org/10.1016/J.WASMAN.2009.09.028.

Duan, B., Zhang, W., Zheng, H., Wu, C., Zhang, Q., Bu, Y., 2017. Disposal Situation of Sewage Sludge from Municipal Wastewater Treatment Plants (WWTPs) and Assessment of the Ecological risk of Heavy Metals for its Land Use in Shanxi, China. Int. J. Environ. Res. Public Health 14, 823. https://doi.org/10.3390/ijerph14070823.

Duan, Z., Yang, W., Zou, S., Liu, H., Zhao, W., Chen, W., 2025. A critical review on cold-bonded artificial aggregate developed from solid wastes: from granulation analysis to performance evaluation. J. Build. Eng. 99, 111588. https://doi.org/10.1016/J.JOBE.2024.111588.

El-Deen, S.E.A.S., Zhang, F., 2012. Synthesis of Sludge@Carbon Nanocomposite for the Recovery of as (V) from Wastewater. Procedia Environ. Sci. 16, 378–390. https://doi.org/10.1016/J.PROENV.2012.10.054.

EN, B.S, 2002. 12457–2, Characterisation of Waste–Leaching–Compliance Test for Leaching of Granular Waste Materials and Sludges. British Standard, UK.

European Environment Agency, 2024. Diversion of waste from landfill in Europe [WWW Document].

European Union, 2024. Statistics | Eurostat [WWW Document]. URL. https://ec.europa.eu/eurostat/databrowser/view/ENV_WW_SPD/default/table?lang=en. (Accessed 21 October 2024).

Ewais, E.M.M., Ahmed, Y.M.Z., El-Amir, A.A.M., El-Didamony, H., 2015. Cement kiln dust–quartz derived wollastonite ceramics. J. Ceram. Soc. Jpn. 123, 527–536. https://doi.org/10.2109/JCERSJ2.123.527.

Fořt, J., Afolayan, A., Medveď, I., Scheinherrová, L., Černý, R., 2024. A review of the role of lightweight aggregates in the development of mechanical strength of concrete. J. Build. Eng. 89, 109312. https://doi.org/10.1016/J.JOBE.2024.109312.

Forth, J.P., Zoorob, S.E., Thanaya, I.N.A., 2015. Development of bitumen-bound waste aggregate building blocks 159, 23–32. https://doi.org/10.1680/COMA.2006.159.1.23.

Franus, M., Barnat-Hunek, D., Wdowin, M., 2016. Utilization of sewage sludge in the manufacture of lightweight aggregate. Environ. Monit. Assess. 188, 1–13. https://doi.org/10.1007/S10661-015-5010-8.

Fytili, D., Zabaniotou, A., 2008. Utilization of sewage sludge in EU application of old and new methods—a review. Renew. Sust. Energ. Rev. 12, 116–140. https://doi.org/10.1016/J.RSER.2006.05.014.

Gao, N., Kamran, K., Quan, C., Williams, P.T., 2020. Thermochemical conversion of sewage sludge: a critical review. Prog. Energy Combust. Sci. 79, 100843. https://doi.org/10.1016/j.pecs.2020.100843.

Garrido-Baserba, M., Molinos-Senante, M., Abelleira-Pereira, J.M., Fdez-Güelfo, L.A., Poch, M., Hernández-Sancho, F., 2015. Selecting sewage sludge treatment alternatives in modern wastewater treatment plants using environmental decision support systems. J. Clean. Prod. 107, 410–419. https://doi.org/10.1016/j.jclepro.2014.11.021.

Geetha, S., Ramamurthy, K., 2010a. Reuse potential of low-calcium bottom ash as aggregate through pelletization. Waste Manag. 30, 1528–1535. https://doi.org/10.1016/J.WASMAN.2010.03.027.

Geetha, S., Ramamurthy, K., 2010b. Environmental friendly technology of cold-bonded bottom ash aggregate manufacture through chemical activation. J. Clean. Prod. 18, 1563–1569. https://doi.org/10.1016/J.JCLEPRO.2010.06.006.

Geng, J., Niu, S., Han, K., Wang, Y., Zhu, J., Yang, Z., Liu, J., Zhang, H., Sun, X., Liang, B., Zheng, Y., 2024. Properties of artificial lightweight aggregates prepared from coal and biomass co-fired fly ashes and sewage sludge fly ash. Ceram. Int. 50, 28609–28618. https://doi.org/10.1016/J.CERAMINT.2024.05.172.

Georgi, K., Ekaterina, S., Alexander, P., Alexander, R., Kirill, Y., Andrey, V., 2022. Sewage sludge as an object of vermicomposting. Bioresour. Technol. Rep. 20, 101281. https://doi.org/10.1016/J.BITEB.2022.101281.

Gesoğlu, M., Güneyisi, E., Öz, H.Ö., 2012. Properties of lightweight aggregates produced with cold-bonding pelletization of fly ash and ground granulated blast furnace slag. Mater. Struct. 45, 1535–1546. https://doi.org/10.1617/s11527-012-9855-9.

Gomathi, P., Anandan, S., 2013. Crushing strength properties of furnace slag-fly ash blended lightweight aggregates. ARPN Journal of Engineering and Applied Sciences 8, 246–251.

Gomathi, P., Sivakumar, A., 2014. Cold Bonded Fly Ash Lightweight Aggregate Containing Different Binders. Res. J. Appl. Sci. Eng. Technol. 7, 1101–1106. https://doi.org/10.19026/RJASET.7.365.

Gomathi, P., Sivakumar, A., 2015. Accelerated curing effects on the mechanical performance of cold bonded and sintered fly ash aggregate concrete. Constr. Build. Mater. 77, 276–287. https://doi.org/10.1016/J.CONBUILDMAT.2014.12.108.

González-Corrochano, B., Alonso-Azcárate, J., Rodas, M., 2009a. Characterization of lightweight aggregates manufactured from washing aggregate sludge and fly ash. Resour. Conserv. Recycl. 53, 571–581. https://doi.org/10.1016/J.RESCONREC.2009.04.008.

González-Corrochano, B., Alonso-Azcárate, J., Rodas, M., 2009b. Production of lightweight aggregates from mining and industrial wastes. J. Environ. Manag. 90, 2801–2812. https://doi.org/10.1016/J.JENVMAN.2009.03.009.

González-Corrochano, B., Alonso-Azcárate, J., Rodríguez, L., Lorenzo, A.P., Torío, M.F., Ramos, J.J.T., Corvinos, M.D., Muro, C., 2016. Valorization of washing aggregate sludge and sewage sludge for lightweight aggregates production. Constr. Build. Mater. 116, 252–262. https://doi.org/10.1016/J.CONBUILDMAT.2016.04.095.

Goto, M., Hidaka, T., Nomura, Y., Fujiwara, T., Park, C., 2025. Effect of solids retention time on wastewater treatment and methane recovery by oxygenic photogranules. Bioresour. Technol. Rep. 31, 102246. https://doi.org/10.1016/J.BITEB.2025.102246.

Government, D. of E. and E. of the AA, 2016. Commonwealth environmental management guidance on perfluorooctane sulfonic acid (PFOS) and perfluorooctanoic acid (PFOA).

Grobelak, A., Stępień, W., Kacprzak, M., 2016. Sewage sludge as an ingredient in fertilizers and soil substitutes. Ecological Engineering & Environmental Technology 2016, 52–60. https://doi.org/10.12912/23920629/63289.

Haddadian, A., Johnson Alengaram, U., Ayough, P., Mo, K.H., Mahmoud Alnahhal, A., 2023. Inherent characteristics of agro and industrial By-Products based lightweight concrete – a comprehensive review. Constr. Build. Mater. 397, 132298. https://doi.org/10.1016/J.CONBUILDMAT.2023.132298.

Hall, A.M., 2021. Long-Term Denudation and Geomorphology in Scotland. In: World Geomorphological Landscapes. Springer Science and Business Media B.V., pp. 41–52. https://doi.org/10.1007/978-3-030-71246-4_3

Harikrishnan, K.I., Ramamurthy, K., 2006. Influence of pelletization process on the properties of fly ash aggregates. Waste Manag. 26, 846–852. https://doi.org/10.1016/J.WASMAN.2005.10.012.

Hasheminezhad, A., King, D., Ceylan, H., Kim, S., 2024. Comparative life cycle assessment of natural and recycled aggregate concrete: a review. Sci. Total Environ. 950, 175310. https://doi.org/10.1016/J.SCITOTENV.2024.175310.

Heap, J.M., Elliott, M., ap Rheinallt, T., 1991. The marine disposal of sewage sludge. Ocean and Shoreline Management 16, 291–312. https://doi.org/10.1016/0951-8312(91)90009-Q.

Hong, Jinglan, Hong, Jingmin, Otaki, M., Jolliet, O., 2009. Environmental and economic life cycle assessment for sewage sludge treatment processes in Japan. Waste Manag. 29, 696–703. https://doi.org/10.1016/j.wasman.2008.03.026.

Huang, C.H., Wang, S.Y., 2013. Application of water treatment sludge in the manufacturing of lightweight aggregate. Constr. Build. Mater. 43, 174–183. https://doi.org/10.1016/J.CONBUILDMAT.2013.02.016.

Hušek, M., Semerád, J., Skoblia, S., Moško, J., Kukla, J., Beňo, Z., Jeremiáš, M., Cajthaml, T., Komárek, M., Pohořelý, M., 2024. Removal of per-and polyfluoroalkyl substances and organic fluorine from sewage sludge and sea sand by pyrolysis. Biochar 6, 31.

International Maritime Organisation(IMO), 2022. Protecting the oceans - ban on disposal at sea of sewage sludge proposed [WWW Document].

Ismail, U.M., Tizaoui, C., 2025. A critical review of per- and polyfluoroalkyl substances (PFAS) in wastewater biosolids and sludge. J. Environ. Chem. Eng. 13, 120422. https://doi.org/10.1016/J.JECE.2025.120422.

Ji, W., Yio, M., Chen, Z., Lu, J.X., Cheeseman, C., Poon, C.S., 2023. Resource recovery of waste glass and incinerated sewage sludge residues in self-foaming lightweight aggregate. Resour. Conserv. Recycl. 199, 107264. https://doi.org/10.1016/J.RESCONREC.2023.107264.

Jo, B. wan, Park, S. kook, Park, J. bin, 2007. Properties of concrete made with alkali-activated fly ash lightweight aggregate (AFLA). Cem. Concr. Compos. 29, 128–135. https://doi.org/10.1016/J.CEMCONCOMP.2006.09.004.

Justin, S., Thushanthan, K., Tharmarajah, G., 2025. Durability and mechanical performance of glass and natural fiber-reinforced concrete in acidic environments. Constr. Build. Mater. 465, 140262. https://doi.org/10.1016/J.CONBUILDMAT.2025.140262.

Kanwar, P., Mina, U., Thakur, I.S., Srivastava, S., 2023. Heavy metal phytoremediation by the novel prospect of microbes, nanotechnology, and genetic engineering for recovery and rehabilitation of landfill site. Bioresour. Technol. Rep. 23, 101518. https://doi.org/10.1016/J.BITEB.2023.101518.

Khanbilvardi, R., Afshari, S., 1995. Sludge Ash as Fine Aggregate for Concrete Mix. J. Environ. Eng. 121, 633–638. https://doi.org/10.1061/(ASCE)0733-9372(1995)121:9(633).

Kockal, N.U., Ozturan, T., 2011. Characteristics of lightweight fly ash aggregates produced with different binders and heat treatments. Cem. Concr. Compos. 33, 61–67. https://doi.org/10.1016/J.CEMCONCOMP.2010.09.007.

Kominko, H., Gorazda, K., Wzorek, Z., 2024. Sewage sludge: a review of its risks and circular raw material potential. J. Water Process Eng. 63, 105522. https://doi.org/10.1016/j.jwpe.2024.105522.

Korol, J., Głodniok, M., Hejna, A., Pawlik, T., Chmielnicki, B., Bondaruk, J., 2020. Manufacturing of lightweight aggregates as an auspicious method of sewage sludge utilization. Materials 13, 5635, 2020. 13, 5635. https://doi.org/10.3390/MA13245635.

Kumar, V., Singh, V., Pandit, S., 2025. Advanced omics approach and sustainable strategies for heavy metal microbial remediation in contaminated environments. Bioresour. Technol. Rep. 29, 102040. https://doi.org/10.1016/J.BITEB.2025.102040.

Latosí Nska, J., Zygadło, M., Czapik, P., 2021. The influence of sewage sludge content and sintering temperature on selected properties of lightweight expanded clay

aggregate. Materials 2021, Vol. 14, Page 3363, 14, 3363. https://doi.org/10.3390/MA14123363.
Lau, P.C., Teo, D.C.L., Mannan, M.A., 2017. Characteristics of lightweight aggregate produced from lime-treated sewage sludge and palm oil fuel ash. Constr. Build. Mater. 152, 558–567. https://doi.org/10.1016/j.conbuildmat.2017.07.022.
Lau, P.C., Teo, D.C.L., Mannan, M.A., 2018. Mechanical, durability and microstructure properties of lightweight concrete using aggregate made from lime-treated sewage sludge and palm oil fuel ash. Constr. Build. Mater. 176, 24–34. https://doi.org/10.1016/J.CONBUILDMAT.2018.04.179.
Laursen, K., White, T.J., Cresswell, D.J.F., Wainwright, P.J., Barton, J.R., 2006. Recycling of an industrial sludge and marine clay as light-weight aggregates. J. Environ. Manag. 80, 208–213. https://doi.org/10.1016/j.jenvman.2005.08.026.
Letcher, R.J., Chu, S., Smyth, S.A., 2020. Side-chain fluorinated polymer surfactants in biosolids from wastewater treatment plants. J. Hazard. Mater. 388. https://doi.org/10.1016/j.jhazmat.2020.122044.
Lewis, A.J., Ebrahimi, F., McKenzie, E.R., Suri, R., Sales, C.M., 2023. Influence of microbial weathering on the partitioning of per-and polyfluoroalkyl substances (PFAS) in biosolids. Environ. Sci. Process Impacts 25, 415–431.
Li, B., Ling, T.-C., Qu, L., Wang, Y., 2016. Effects of a two-step heating process on the properties of lightweight aggregate prepared with sewage sludge and saline clay. Constr. Build. Mater. 114, 119–126. https://doi.org/10.1016/j.conbuildmat.2016.03.159.
Li, D., Wang, Y., Liu, Y., Sun, S., Gao, Y., 2020. Estimating life-cycle CO2 emissions of urban road corridor construction: a case study in Xi'an, China. J. Clean. Prod. 255, 120033. https://doi.org/10.1016/J.JCLEPRO.2020.120033.
Li, X., He, C., Lv, Y., Jian, S., Liu, G., Jiang, W., Jiang, D., 2020a. Utilization of municipal sewage sludge and waste glass powder in production of lightweight aggregates. Constr. Build. Mater. 256, 119413. https://doi.org/10.1016/j.conbuildmat.2020.119413.
Li, X., He, C., Lv, Y., Jian, S., Liu, G., Jiang, W., Jiang, D., 2020b. Utilization of municipal sewage sludge and waste glass powder in production of lightweight aggregates. Constr. Build. Mater. 256, 119413. https://doi.org/10.1016/J.CONBUILDMAT.2020.119413.
Li, X., He, C., Lv, Y., Jian, S., Jiang, W., Jiang, D., Wu, K., Dan, J., 2021. Effect of sintering temperature and dwelling time on the characteristics of lightweight aggregate produced from sewage sludge and waste glass powder. Ceram. Int. 47, 33435–33443. https://doi.org/10.1016/J.CERAMINT.2021.08.250.
Li, Y., Zhang, J., 2021. Exposure to lead and cadmium of the Belgian consumers from ceramic food contact articles. Toxicol. Rep. 8, 548–556. https://doi.org/10.1016/j.toxrep.2021.02.015.
Liao, Y.C., Huang, C.Y., 2011. Effects of heat treatment on the physical properties of lightweight aggregate from water reservoir sediment. Ceram. Int. 37, 3723–3730. https://doi.org/10.1016/J.CERAMINT.2011.04.122.
Lima, J.F., Ingunza, D., Quiñones Klinger, M.D.P., 2015. Effects of Sewage Sludge Ashes Addition in Portland Cement Concretes 189–191. https://doi.org/10.2991/cmes-15.2015.55.
Liu, J., Liu, R., He, Z., Ba, M., Li, Y., 2012. Preparation and microstructure of green ceramsite made from sewage sludge. Journal Wuhan University of Technology, Materials Science Edition 27, 149–153. https://doi.org/10.1007/S11595-012-0426-2/METRICS.
Liu, M., Xu, G., Li, G., 2017. Effect of the ratio of components on the characteristics of lightweight aggregate made from sewage sludge and river sediment. Process. Saf. Environ. Prot. 105, 109–116. https://doi.org/10.1016/J.PSEP.2016.10.018.
Liu, M., Liu, X., Wang, W., Guo, J., Zhang, L., Zhang, H., 2018a. Effect of SiO2 and Al2O3 on characteristics of lightweight aggregate made from sewage sludge and river sediment. Ceram. Int. 44, 4313–4319. https://doi.org/10.1016/J.CERAMINT.2017.12.022.
Liu, M., Wang, C., Bai, Y., Xu, G., 2018b. Effects of sintering temperature on the characteristics of lightweight aggregate made from sewage sludge and river sediment. J. Alloys Compd. 748, 522–527. https://doi.org/10.1016/J.JALLCOM.2018.03.216.
Liu, Y., Zhou, S., Liu, R., Chen, M., Xu, J., Liao, M., Tu, W., Tang, P., 2022. Utilization of waste sludge: Activation/modification methods and adsorption applications of sludge-based activated carbon. J. Water Process Eng. 49, 103111. https://doi.org/10.1016/J.JWPE.2022.103111.
Lo, T.Y., Cui, H., Memon, S.A., Noguchi, T., 2016. Manufacturing of sintered lightweight aggregate using high-carbon fly ash and its effect on the mechanical properties and microstructure of concrete. J. Clean. Prod. 112, 753–762. https://doi.org/10.1016/j.jclepro.2015.07.001.
Magdziarz, A., Wilk, M., Kosturkiewicz, B., 2011. Investigation of sewage sludge preparation for combustion process. Chem. Process. Eng. 32. https://doi.org/10.2478/v10176-011-0024-4.
Mahadevan, P., 2019. Sand mafias in India. In: Disorganized Crime in a Growing Economy, pp. 1–27.
Manikandan, R., Ramamurthy, K., 2007. Influence of fineness of fly ash on the aggregate pelletization process. Cem. Concr. Compos. 29, 456–464. https://doi.org/10.1016/J.CEMCONCOMP.2007.01.002.
Massa, M., Calce, S., Pachaiappan, P., Valentim, B., Punta, C., D'Anna, A., Blazina, M., Bontempi, E., 2025. Exploring the potential of sewage sludge ash for CO2 sequestration and resource recovery. J. Water Process Eng. 71, 107153. https://doi.org/10.1016/J.JWPE.2025.107153.
Mateo-Sagasta, J., Raschid-Sally, L., Thebo, A., 2015. Global Wastewater and Sludge Production, Treatment and Use. In: Wastewater: Economic Asset in an Urbanizing World, pp. 15–38. https://doi.org/10.1007/978-94-017-9545-6_2.
McNamara, P., Samuel, M.S., Sathyamoorthy, S., Moss, L., Valtierra, D., Cortes Lopez, H., Nigro, N., Somerville, S., Liu, Z., 2022. Pyrolysis transports, and transforms, PFAS from biosolids to py-liquid. Environ Sci (Camb) 9, 386–395. https://doi.org/10.1039/d2ew00677d.
Meena, R.A.A., Yukesh Kannah, R., Sindhu, J., Ragavi, J., Kumar, G., Gunasekaran, M., Rajesh Banu, J., 2019. Trends and resource recovery in biological wastewater treatment system. Bioresour. Technol. Rep. 7, 100235. https://doi.org/10.1016/J.BITEB.2019.100235.
Min Wie, Y., Hyuck Lee, K., Gang Lee, K., Park, J., Ko, T., Hoon Lee, K., 2023. Manufacture of artificial lightweight aggregates recycled from anaerobic digested sewage sludge and process optimization by machine learning modeling techniques. Constr. Build. Mater. 399, 132502. https://doi.org/10.1016/J.CONBUILDMAT.2023.132502.
Mineral Products Association, 2017. Long-term Aggregates Demand & Supply Scenarios, 2016–30.
Mininni, G., Blanch, A.R., Lucena, F., Berselli, S., 2015. EU policy on sewage sludge utilization and perspectives on new approaches of sludge management. Environ. Sci. Pollut. Res. 22, 7361–7374. https://doi.org/10.1007/s11356-014-3132-0.
Mohanta, N.R., Murmu, M., 2022. Alternative coarse aggregate for sustainable and eco-friendly concrete - a review. J. Build. Eng. 59, 105079. https://doi.org/10.1016/J.JOBE.2022.105079.
Molenda, M., Horabik, J., Parafiniuk, P., Oniszczuk, A., Bá Nda, M., Wajs, J., Gondek, E., Chutkowski, M., Lisowski, A., Wi, J., Acek, ˛., Stasiak, M., 2021. Materials Mechanical and Combustion Properties of Agglomerates of Wood of Popular Eastern European Species. https://doi.org/10.3390/ma14112728.
Moodie, D., Coggan, T., Berry, K., Kolobaric, A., Fernandes, M., Lee, E., Reichman, S., Nugegoda, D., Clarke, B.O., 2021. Legacy and emerging per- and polyfluoroalkyl substances (PFASs) in Australian biosolids. Chemosphere 270. https://doi.org/10.1016/j.chemosphere.2020.129143.
Mun, K.J., 2007. Development and tests of lightweight aggregate using sewage sludge for nonstructural concrete. Constr. Build. Mater. 21, 1583–1588. https://doi.org/10.1016/j.conbuildmat.2005.09.009.
National Oceanic and Atmospheric Administration(NOAA), 2001. Studying Deep-sea Biodiversity and Dumping [WWW Document].
OECD, 2019. Material Resources Outlook to 2060: Economic Drivers and Environmental Consequences. OECD publishing.
Okeke, E.S., Okoye, C.O., Atakpa, E.O., Ita, R.E., Nyaruaba, R., Mgbechidinma, C.L., Akan, O.D., 2022. Microplastics in agroecosystems-impacts on ecosystem functions and food chain. Resour. Conserv. Recycl. 177, 105961. https://doi.org/10.1016/J.RESCONREC.2021.105961.
Othuman, M.A., Wang, Y.C., 2011. Elevated-temperature thermal properties of lightweight foamed concrete. Constr. Build. Mater. 25, 705–716. https://doi.org/10.1016/J.CONBUILDMAT.2010.07.016.
Peduzzi, P., Peduzzi, Pascal, 2014. Sand, rarer than one thinks. Environ. Dev. 11, 208–218. https://doi.org/10.1016/j.envdev.2014.04.001.
Piippo, S., Lauronen, M., Postila, H., 2018. Greenhouse gas emissions from different sewage sludge treatment methods in north. J. Clean. Prod. 177, 483–492. https://doi.org/10.1016/J.JCLEPRO.2017.12.232.
Poblete, R., Çelik, G., Salihoglu, N.K., 2025. Water recovery and reuse as a strategy for sustainable compost management. Bioresour. Technol. Rep. 30, 102164. https://doi.org/10.1016/J.BITEB.2025.102164.
Poinen, P., Bokhoree, C., 2022. Sludge management practices: Drivers, opportunities and implications for small island developing states. J. Water Process Eng. 48, 102860. https://doi.org/10.1016/J.JWPE.2022.102860.
Praspaliauskas, M., Pedišius, N., 2017. A review of sludge characteristics in Lithuania's wastewater treatment plants and perspectives of its usage in thermal processes. Renew. Sust. Energ. Rev. 67, 899–907. https://doi.org/10.1016/j.rser.2016.09.041.
Ragi, K.B., Ekka, B., Mezule, L., 2022. Zero pollution protocol for the recovery of cellulose from municipal sewage sludge. Bioresour. Technol. Rep. 20, 101222. https://doi.org/10.1016/J.BITEB.2022.101222.
Rajput, N.A., Laghari, M., Mangio, H. ur R., Soothar, R.K., 2024. Enhanced phosphorus and potassium recovery through co-pyrolysis of nutrient-rich biomass feedstocks for engineered biochar production. Bioresour. Technol. Rep. 26, 101818. https://doi.org/10.1016/J.BITEB.2024.101818.
Ramadan, M., Fouad, H., Hassanain, A., 2008. Reuse of water treatment plant sludge in brick manufacturing. J. Appl. Sci. Res. 4 (10), 1223–1229.
Ramamurthy, K., Harikrishnan, K.I., 2006. Influence of binders on properties of sintered fly ash aggregate. Cem. Concr. Compos. 28, 33–38. https://doi.org/10.1016/J.CEMCONCOMP.2005.06.005.
Rashad, A.M., 2018. Lightweight expanded clay aggregate as a building material – an overview. Constr. Build. Mater. 170, 757–775. https://doi.org/10.1016/J.CONBUILDMAT.2018.03.009.
Ren, P., Ling, T.C., Mo, K.H., 2021. Recent advances in artificial aggregate production. J. Clean. Prod. 291, 125215. https://doi.org/10.1016/J.JCLEPRO.2020.125215.
Richman, T., Arnold, E., Williams, A.J., 2022. Curation of a list of chemicals in biosolids from EPA national sewage sludge surveys & biennial review reports. Sci. Data 9. https://doi.org/10.1038/S41597-022-01267-9.
Riley, C.M., 1951. Relation of Chemical Properties to the Bloating of Clays. J. Am. Ceram. Soc. 34, 121–128. https://doi.org/10.1111/J.1151-2916.1951.TB11619.X.
Risdanareni, P., Schollbach, K., Wang, J., De Belie, N., 2020. The effect of NaOH concentration on the mechanical and physical properties of alkali activated fly ash-based artificial lightweight aggregate. Constr. Build. Mater. 259, 119832. https://doi.org/10.1016/J.CONBUILDMAT.2020.119832.
Rossignolo, J.A., 2009. Concreto leve estrutural: produção, propriedades, microestrutura e aplicações. Pini.
Ruimin, Y., Zhenning, Z., Zihao, F.A.N., Lu, S., Jinhui, L.I., Bang, Z., 2021. Effect of organic content on compression properties of municipal sewage sludge. IOP Conf.

Ser. Earth Environ. Sci. 643, 012105. https://doi.org/10.1088/1755-1315/643/1/012105.
Sakali, A., Coello, D., Haïlaf, A., Egea-Corbacho, A., Albendín, G., Arellano, J., Brigui, J., Quiroga, J.M., Rodríguez-Barroso, R., 2021. A new protocol to assess the microplastics in sewage sludge. J. Water Process Eng. 44, 102344. https://doi.org/10.1016/J.JWPE.2021.102344.
Sánchez, A.S., Martins, G., 2021. Nutrient recovery in wastewater treatment plants: Comparative assessment of different technological options for the metropolitan region of Buenos Aires. J. Water Process Eng. 41, 102076. https://doi.org/10.1016/J.JWPE.2021.102076.
Saunders, D.L., Meeuwig, J.J., Vincent, A.C.J., 2002. Freshwater protected areas: strategies for conservation. Conserv. Biol. 16, 30–41. https://doi.org/10.1046/J.1523-1739.2002.99562.X.
Schlederer, F., Martín-Hernández, E., Vaneeckhaute, C., 2024. On safety of sewage biosolids valorisation: distribution of PFAS, PAHs, PCDD/Fs, and heavy metals in low-temperature pyrolysis end-products for agricultural and energetic applications. Chem. Eng. J. 498, 155534.
Seleiman, M.F., Santanen, A., Mäkelä, P.S.A., 2020. Recycling sludge on cropland as fertilizer – Advantages and risks. Resour. Conserv. Recycl. 155, 104647. https://doi.org/10.1016/J.RESCONREC.2019.104647.
Shi, M., Ling, T.C., Gan, B., Guo, M.Z., 2019. Turning concrete waste powder into carbonated artificial aggregates. Constr. Build. Mater. 199, 178–184. https://doi.org/10.1016/J.CONBUILDMAT.2018.12.021.
Shivaprasad, K.N., Das, B.B., 2021. Study on the production factors in the process of production and properties of fly ash-based coarse aggregates. Adv. Civil Eng. 2021. https://doi.org/10.1155/2021/4309569.
Sidhu, A.S., Siddique, R., Singh, G., 2024. Review on the effect of sewage sludge ash on the properties of concrete. Constr. Build. Mater. 449, 138296. https://doi.org/10.1016/j.conbuildmat.2024.138296.
Silva, R.D.V.K., Lei, Z., Shimizu, K., Zhang, Z., 2020. Hydrothermal treatment of sewage sludge to produce solid biofuel: Focus on fuel characteristics. Bioresour. Technol. Rep. 11, 100453. https://doi.org/10.1016/J.BITEB.2020.100453.
Sørmo, E., Castro, G., Hubert, M., Licul-Kucera, V., Quintanilla, M., Asimakopoulos, A.G., Cornelissen, G., Arp, H.P.H., 2023. The decomposition and emission factors of a wide range of PFAS in diverse, contaminated organic waste fractions undergoing dry pyrolysis. J. Hazard. Mater. 454, 131447.
Souza, M.M., Anjos, M.A.S., Sá, M.V.V.A., Souza, N.S.L., 2020. Developing and classifying lightweight aggregates from sewage sludge and rice husk ash. Case Stud. Constr. Mater. 12, e00340. https://doi.org/10.1016/J.CSCM.2020.E00340.
Stahl, T., Gassmann, M., Falk, S., Brunn, H., 2018. In: Stahl, T., Gassmann, M., Falk, S., Brunn, H. (Eds.), Concentrations and Distribution Patterns of Perfluoroalkyl Acids in Sewage sludge and in biowaste in Hesse, 66. Journal of agricultural and food chemistry, 2018•ACS Publications, Germany. ACS Publications, pp. 10147–10153. https://doi.org/10.1021/ACS.JAFC.8B03063.
Suresh, G., Kumar, P., Jayakumar, K., 2016a. Effect of GGBS and Fly ash aggregates on properties of geopolymer concrete. J. Struct. Eng. 43, 436–444.
Suresh, G.V., Reddy, P.P.K., Karthikeyan, J., 2016b. Effect of GGBS & fly ash aggregates on properties of geopolymer concrete. J. Struct. Eng. 43, 436–444.
Świerczek, L., Cieślik, B.M., Konieczka, P., 2018. The potential of raw sewage sludge in construction industry – a review. J. Clean. Prod. 200, 342–356. https://doi.org/10.1016/j.jclepro.2018.07.188.
Tajra, F., Elrahman, M.A., Chung, S.Y., Stephan, D., 2018. Performance assessment of core-shell structured lightweight aggregate produced by cold bonding pelletization process. Constr. Build. Mater. 179, 220–231. https://doi.org/10.1016/J.CONBUILDMAT.2018.05.237.
Taki, K., Gahlot, R., Kumar, M., 2020. Utilization of fly ash amended sewage sludge as brick for sustainable building material with special emphasis on dimensional effect. J. Clean. Prod. 275, 123942. https://doi.org/10.1016/j.jclepro.2020.123942.
Tang, P., Xuan, D., Cheng, H.W., Poon, C.S., Tsang, D.C.W., 2020. Use of CO2 curing to enhance the properties of cold bonded lightweight aggregates (CBLAs) produced with concrete slurry waste (CSW) and fine incineration bottom ash (IBA). J. Hazard. Mater. 381, 120951. https://doi.org/10.1016/J.JHAZMAT.2019.120951.
Tang, P., Jiang, S., Chen, W., Deng, T., 2023. Self-foaming high strength artificial lightweight aggregates derived from solid wastes: expansion mechanism and environmental impact. Constr. Build. Mater. 370, 130698. https://doi.org/10.1016/J.CONBUILDMAT.2023.130698.
Thukkaram, S., Arun Kumar, A., 2024. Behaviour of sewage sludge based lightweight aggregate in geopolymer concrete. Mater. Res. Express 11, 055501. https://doi.org/10.1088/2053-1591/ad4198.
Tian, K., Wang, Y., Hong, S., Zhang, J., Hou, D., Dong, B., Xing, F., 2021. Alkali-activated artificial aggregates fabricated by red mud and fly ash: Performance and microstructure. Constr. Build. Mater. 281, 122552. https://doi.org/10.1016/j.conbuildmat.2021.122552.
Tian, Y., Dai, S., Wang, J., 2023. Environmental standards and beneficial uses of waste-to-energy (WTE) residues in civil engineering applications. Waste Disposal & Sustainable Energy 5:3 (5), 323–350. https://doi.org/10.1007/S42768-023-00140-8, 2023.
Torri, S.I., Lavado, R.S., 2008. Dynamics of Cd, Cu and Pb added to soil through different kinds of sewage sludge. Waste Manag. 28, 821–832. https://doi.org/10.1016/j.wasman.2007.01.020.
Torri, S.I., Corrêa, R.S., Renella, G., 2014. Soil Carbon Sequestration Resulting from Biosolids Application. Appl. Environ. Soil Sci. 2014, 821768. https://doi.org/10.1155/2014/821768.
Tsai, Y.-C., Li, Y.-C., 2012. Test anxiety and Foreign Language Reading anxiety in a Reading-Proficiency Test. Journal of Social Sciences 8, 95–103. https://doi.org/10.3844/JSSP.2012.95.103.
Tuan, B.L.A., Hwang, C.-L., Lin, K.-L., Chen, Y.-Y., Young, M.-P., 2013. Development of lightweight aggregate from sewage sludge and waste glass powder for concrete. Constr. Build. Mater. 47, 334–339. https://doi.org/10.1016/j.conbuildmat.2013.05.039.
Tuncel, E.Y., Pekmezci, B.Y., 2018. A sustainable cold bonded lightweight PCM aggregate production: its effects on concrete properties. Constr. Build. Mater. 181, 199–216. https://doi.org/10.1016/J.CONBUILDMAT.2018.05.269.
UNEP, Schandl, H., Fischer-Kowalski, M., West, J., Giljum, S., Dittrich, M., Eisenmenger, N., Geschke, A., Lieber, M., Wieland, H., Schaffartzik, A., Krausmann, F., Gierlinger, S., Hosking, K., Lenzen, M., Tanikawa, H., Miatto, A., Fishman, T., 2016. Global Material Flows and Resource Productivity. An Assessment Study of the UNEP International Resource Panel.
Vasugi, V., Ramamurthy, K., 2014. Identification of admixture for pelletization and strength enhancement of sintered coal pond ash aggregate through statistically designed experiments. Mater. Des. 60, 563–575. https://doi.org/10.1016/j.matdes.2014.04.023.
Venkatesan, A.K., Halden, R.U., 2013. National inventory of perfluoroalkyl substances in archived U.S. biosolids from the 2001 EPA National Sewage Sludge Survey. J. Hazard. Mater. 252–253, 413–418. https://doi.org/10.1016/j.jhazmat.2013.03.016.
Wainwright, P.J., Cresswell, D.J.F., 2001. Synthetic aggregates from combustion ashes using an innovative rotary kiln. Waste Manag. 21, 241–246. https://doi.org/10.1016/S0956-053X(00)00096-9.
Wang, B., Xiao, J., Zheng, Z., Gan, W., Shen, J., Wang, J., 2025. Assessment of construction spoil generation: a case study in China. J. Clean. Prod. 532, 146879. https://doi.org/10.1016/J.JCLEPRO.2025.146879.
Wang, H., Xu, W., Sharif, M., Cheng, G., Zhang, Z., 2022. Resource utilization of solid waste carbide slag: a brief review of application technologies in various scenes. Waste Dispos Sustain Energy 4, 1–16. https://doi.org/10.1007/S42768-021-00090-Z/METRICS.
Wang, T., Zhang, J., Xu, Y., 2020. Epigenetic Basis of Lead-Induced Neurological Disorders. Int. J. Environ. Res. Public Health 17, 1–23. https://doi.org/10.3390/IJERPH17134878.
Wang, X., Jin, Y., Wang, Z., Mahar, R.B., Nie, Y., 2008. A research on sintering characteristics and mechanisms of dried sewage sludge. J. Hazard. Mater. 160, 489–494. https://doi.org/10.1016/J.JHAZMAT.2008.03.054.
Wang, X., Jin, Y., Wang, Z., Nie, Y., Huang, Q., Wang, Q., 2009a. Development of lightweight aggregate from dry sewage sludge and coal ash. Waste Manag. 29, 1330–1335. https://doi.org/10.1016/J.WASMAN.2008.09.006.
Wang, X., Jin, Y., Wang, Z., Nie, Y., Huang, Q., Wang, Q., 2009b. Development of lightweight aggregate from dry sewage sludge and coal ash. Waste Manag. 29, 1330–1335. https://doi.org/10.1016/j.wasman.2008.09.006.
Water UK, 2025. Extracting resources from sewage [WWW Document]. URL. https://www.water.org.uk/waste-water/extracting-resources-sewage. (Accessed 21 October 2024).
Winchell, L.J., Cullen, J., Ross, J.J., Seidel, A., Romero, M. Lou, Kakar, F., Bronstad, E., Wells, M.J.M., Klinghoffer, N.B., Berruti, F., 2024. Fate of biosolids-bound PFAS through pyrolysis coupled with thermal oxidation for air emissions control. Water Environ. Res. 96, e11149.
Xiao, J., 2018. Recycled Aggregate Concrete Structures. Springer Tracts in Civil Engineering. https://doi.org/10.1007/978-3-662-53987-3.
Xiao, J., Jiang, Y., Wang, D., Noguchi, T., Lu, Z., 2025. Global CO2 sequestration potential of recycled aggregates: Modeling, life cycle analysis, and accelerated carbonation strategies. Waste Manag. 204, 114951. https://doi.org/10.1016/J.WASMAN.2025.114951.
Xu, G., Zou, J., Li, G., 2008. Ceramsite made with water and wastewater sludge and its characteristics affected by SiO2 and Al2O3. Environ. Sci. Technol. 42, 7417–7423. https://doi.org/10.1021/ES801446H/SUPPL_FILE/ES801446H_SI_001.PDF.
Xu, G.R., Zou, J.L., Dai, Y., 2006. Utilization of dried sludge for making ceramsite. Water Sci. Technol. 54, 69–79. https://doi.org/10.2166/WST.2006.755.
Xue, J., Verstraete, W., Ni, B.J., Giesy, J.P., Kaur, G., Jiang, D., McBean, E., Li, Z., Shin, H.M., Xiao, F., Liu, Y., Liu, J., Chibwe, L., Wai Ng, K.T., Uchida, Y., 2025. Rethink biosolids: risks and opportunities in the circular economy. Chem. Eng. J. 510, 161749. https://doi.org/10.1016/J.CEJ.2025.161749.
Yang, F., Zhou, W., Zhu, R., Dai, G., W.W.-J. of C, 2021a. Synergistic effects of amorphous porous materials and anhydrous Na2CO3 on the performance of bricks with high municipal sewage sludge content. J. Clean. Prod. 280, 124338. https://doi.org/10.1016/j.jclepro.2020.124338 undefined, 2023.
Yang, F., Zhou, W., Zhu, R., Dai, G., Wang, Weijie, Wang, Wenlong, Guo, X., Jiang, J., Wang, Z., 2021b. Synergistic effects of amorphous porous materials and anhydrous Na2CO3 on the performance of bricks with high municipal sewage sludge content. J. Clean. Prod. 280, 124338. https://doi.org/10.1016/J.JCLEPRO.2020.124338.
Yang, S.-J., Eom, J.-Y., Lee, M.-J., Hwang, D.-H., Park, W.-B., Wie, Y.-M., Lee, K.-G., Lee, K.-H., Yang, S.-J., Eom, J.-Y., Lee, M.-J., Hwang, D.-H., Park, W.-B., Wie, Y.-M., Lee, K.-G., Lee, K.-H., 2023. Comparative environmental evaluation of sewage sludge treatment and aggregate production process by life cycle assessment. Sustainability 16 (16). https://doi.org/10.3390/SU16010226, 2024.
Yang, W., Song, W., Li, J., Zhang, X., 2020. Bioleaching of heavy metals from wastewater sludge with the aim of land application. Chemosphere 249, 126134. https://doi.org/10.1016/j.chemosphere.2020.126134.
Ye, Y., Hao Ngo, H., Guo, W., Woong Chang, S., Duc Nguyen, D., Fu, Q., Wei, W., Ni, B., Cheng, D., Liu, Y., 2022. A critical review on utilization of sewage sludge as environmental functional materials. Bioresour. Technol. 363, 127984. https://doi.org/10.1016/j.biortech.2022.127984.
Yu, L., Zhang, Y., Zhang, Z., Mao, H., Han, H., Yang, J., 2023. Recycling reuse of municipal sewage sludge in sustainable structural materials: Preparation, properties,

crystallization and microstructure analyses. Constr. Build. Mater. 398, 132507. https://doi.org/10.1016/J.CONBUILDMAT.2023.132507.
Yue, M., Yue, Q., Qi, Y., 2011a. Effect of Sintering Temperature on the Properties of Sludge Ceramics and Fly-Ash Ceramics. Adv. Mater. Res. 150–151, 1068–1072. https://doi.org/10.4028/WWW.SCIENTIFIC.NET/AMR.150-151.1068.
Yue, M., Yue, Q.Y., Qi, Y.F., 2011b. Effect of Sintering Temperature on the Properties of Sludge Ceramics and Fly-Ash Ceramics. Adv. Mater. Res. 150–151, 1068–1072. https://doi.org/10.4028/www.scientific.net/AMR.150-151.1068.
Zhang, S., Liu, L., Tan, K., Zhang, L., Tang, K., 2015. Influence of burning temperature and cooling methods on strength of high carbon ferrochrome slag lightweight aggregate. Constr. Build. Mater. 93, 1180–1187. https://doi.org/10.1016/j.conbuildmat.2015.04.045.
Zhang, Y., Yu, L., Wang, J., Mao, H., Cui, K., 2022. Microstructure and mechanical properties of high strength porous ceramics with high sewage sludge content. J. Clean. Prod. 380, 135084. https://doi.org/10.1016/J.JCLEPRO.2022.135084.
Zheng, G., Koziński, J.A., 2000. Thermal events occurring during the combustion of biomass residue. Fuel 79, 181–192. https://doi.org/10.1016/S0016-2361(99)00130-1.
Zhou, T., Li, X., Liu, H., Dong, S., Zhang, Z., Wang, Z., Li, J., Nghiem, L.D., Khan, S.J., Wang, Q., 2024. Occurrence, fate, and remediation for per-and polyfluoroalkyl substances (PFAS) in sewage sludge: a comprehensive review. J. Hazard. Mater. 466, 133637. https://doi.org/10.1016/J.JHAZMAT.2024.133637.